Received: 13 October 2023 | Revised: 3 April 2024 | Accepted: 9 April 2024

DOI: 10.1002/dvdy.712

RESEARCH ARTICLE

Developmental Dynamics WILEY

Muscular remodeling and anteroposterior patterning during tapeworm segmentation

Francesca Jarero[1,2] | **Andrew Baillie**[1] | **Nick Riddiford**[1] | **Jimena Montagne**[3] | **Uriel Koziol**[3] | **Peter D. Olson**[1]

[1]Department of Life Sciences, Natural History Museum, London, UK

[2]Department of Genetics, Evolution and Environment, University College, London, UK

[3]Sección Biología Celular, Facultad de Ciencias, Universidad de la República, Montevideo, Uruguay

Correspondence
Peter D. Olson, Department of Life Sciences, Natural History Museum, London SW7 5BD, UK.
Email: p.olson@nhm.ac.uk

Uriel Koziol, Sección Biología Celular, Facultad de Ciencias, Universidad de la República, Montevideo, Uruguay.
Email: ukoziol@fcien.edu.uy

Funding information
Natural History Museum and University College London

Abstract

Background: Tapeworms are parasitic flatworms that independently evolved a segmented body plan, historically confounding comparisons with other animals. Anteroposterior (AP) patterning in free-living flatworms and in tapeworm larvae is associated with canonical Wnt signaling and positional control genes (PCGs) are expressed by their musculature in regionalized domains along the AP axis. Here, we extend investigations of PCG expression to the adult of the mouse bile-duct tapeworm *Hymenolepis microstoma*, focusing on the growth zone of the neck region and the initial establishment of segmental patterning.

Results: We show that the adult musculature includes new, segmental elements that first appear in the neck and that the spatial patterns of Wnt factors are consistent with expression by muscle cells. Wnt factor expression is highly regionalized and becomes AP-polarized in segments, marking them with axes in agreement with the polarity of the main body axis, while the transition between the neck and strobila is specifically demarcated by the expression domain of a Wnt11 paralog.

Conclusion: We suggest that segmentation could originate in the muscular system and participate in patterning the AP axis through regional and polarized expression of PCGs, akin to the gene regulatory networks employed by free-living flatworms and other animals.

KEYWORDS

anteroposterior patterning, Cestoda, hedgehog, Platyhelminthes, positional control genes, Wnt

1 | INTRODUCTION

Tapeworms are a medically and economically important group of helminth pathogens and one of the oldest recognized forms of parasitic worms.[1] Their segmented, or strobilar, adult body plan is a derived feature not only among flatworms (phylum Platyhelminthes) but also among members of the class Cestoda in which repetition of body parts appears to have evolved in a step-wise fashion under selection for increased fecundity.[2] Their

multi-host life cycles and highly derived form lacking most cephalized structures as well as a gut has made their body plan difficult to homologize with other animals[3–5] leaving longstanding questions regarding the true polarity of their anteroposterior (AP) axis,[6–8] the individuality of their segments[9] and more generally whether the mechanisms that underlie segmentation resemble those of other animals.[10,11]

Canonical Wnt signaling is a universal form of cell–cell communication in Metazoa with a conserved function in AP patterning through the combination of posterior Wnt signaling and anterior Wnt inhibition.[12] AP patterning in free-living planarian flatworms is also regulated by canonical, β-catenin-dependent Wnt signaling[13] and expression of ligands, inhibitors and receptors show distinct regionalization along the main body axis.[14] These and other region-specific markers have been referred to as positional control genes (PCGs) and are expressed continuously by muscle cells throughout their lives,[15,16] maintaining an axial Cartesian coordinate system[17] that is instructive to the somatic stem cells (neoblasts) responsible for all cellular renewal during growth, homeostasis and regeneration.

Extending this model to parasitic flatworms, Koziol et al.[5] investigated the expression domains of Wnt components[18] and other canonical markers of AP patterning during larval metamorphosis in two tapeworm species with highly disparate morphologies. For the first time this provided a common basis of comparison and showed that despite gross morphological differences in the structure of their larvae, in both species the site(s) of scolex formation (i.e., the "head" containing the holdfast structures and the central nervous system [CNS]), is preceded by expression of Wnt inhibitors, whereas the larval cyst tissues, which have evolved into a diverse range of morphologies in different tapeworm groups,[19] express posterior markers including canonical Wnt ligands. This resolved the question of the true developmental AP polarity of the larval worm and provided support for the idea that metamorphosis represents the phylotypic stage in their ontogeny, with AP-regionalized patterns of Wnt expression mirrored across different larval forms of tapeworms and planarians.[5] It also demonstrated PCG expression in tapeworm muscle cells. However, the pattern of Wnt expression during adult development, including questions regarding the polarity of the individual segments, are still unknown.[7,8]

Metamorphosis of the tapeworm oncosphere results in the genesis of an encysted, juvenile worm with a fully developed scolex and body that includes all major elements of the muscle, nerve and osmoregulatory systems (Figure 1). In most tapeworms, sexual and strobilar development are repressed until the larva is transmitted to the enteric system of the vertebrate, final host in which the larvae lose their cyst tissues before becoming established in the small intestine (and bile duct in the case of *Hymenolepis microstoma*). Adult development then commences via elongation of the body with the germinative neck region and strobila intercalated between the scolex and the posterior end of the juvenile worm (Figure 1A). Sexual development is coupled to segmentation and results in the continual production of hermaphroditic sets of reproductive organs (proglottids) that are superficially separated by segmental elements of the musculature. Adult development thus represents the second major transformation in their postembryonic ontogeny and a significant departure from the typical, non-segmented flatworm body plan.

Throughout these developmental processes, cell proliferation is restricted to a population of undifferentiated stem cells, known as germinative cells, that are akin to the neoblasts of planarians and other flatworms.[4] In adult tapeworms these cells are absent from the cortical tissues, being restricted to the periphery of the medullary (inner) parenchyma, and in the central region where they contribute to the development of the reproductive organs (Figure 1E, Additional files 1–3). Germinative cell populations are found in these locations throughout the length of the worm and are not restricted to a specific region such as the neck.

Here, we extend investigations of PCG expression during larval metamorphosis to the strobilar phase of the life cycle of the mouse bile-duct tapeworm *H. microstoma*,[20] concentrating on the neck region and initial segmental patterning of the adult body, prior to maturation of the reproductive organs. This classical mouse/beetle-hosted laboratory system has been the subject of genomic,[21–24] transcriptomic,[25,26] and developmental studies[5,27,28] that underpin its utility as a contemporary model and is supported by a complete, chromosome-level assembly of its genome.[29] We show that adult development begins with the formation of segmentally arranged elements of the muscular system in the neck that subsequently come to define segment boundaries. Wnt components are expressed in muscular domains that become AP-polarized in the transition between the neck and strobila, a region that is uniquely marked by the expression of a Wnt11 gene. In the strobila, polarized expression of inhibitors and ligands mark individual segments with AP poles in agreement with the polarity of the main body axis. Together our results suggest that segmentation in tapeworms could originate in the muscular system and participate in patterning the AP axis through regional and polarized expression of PCGs.

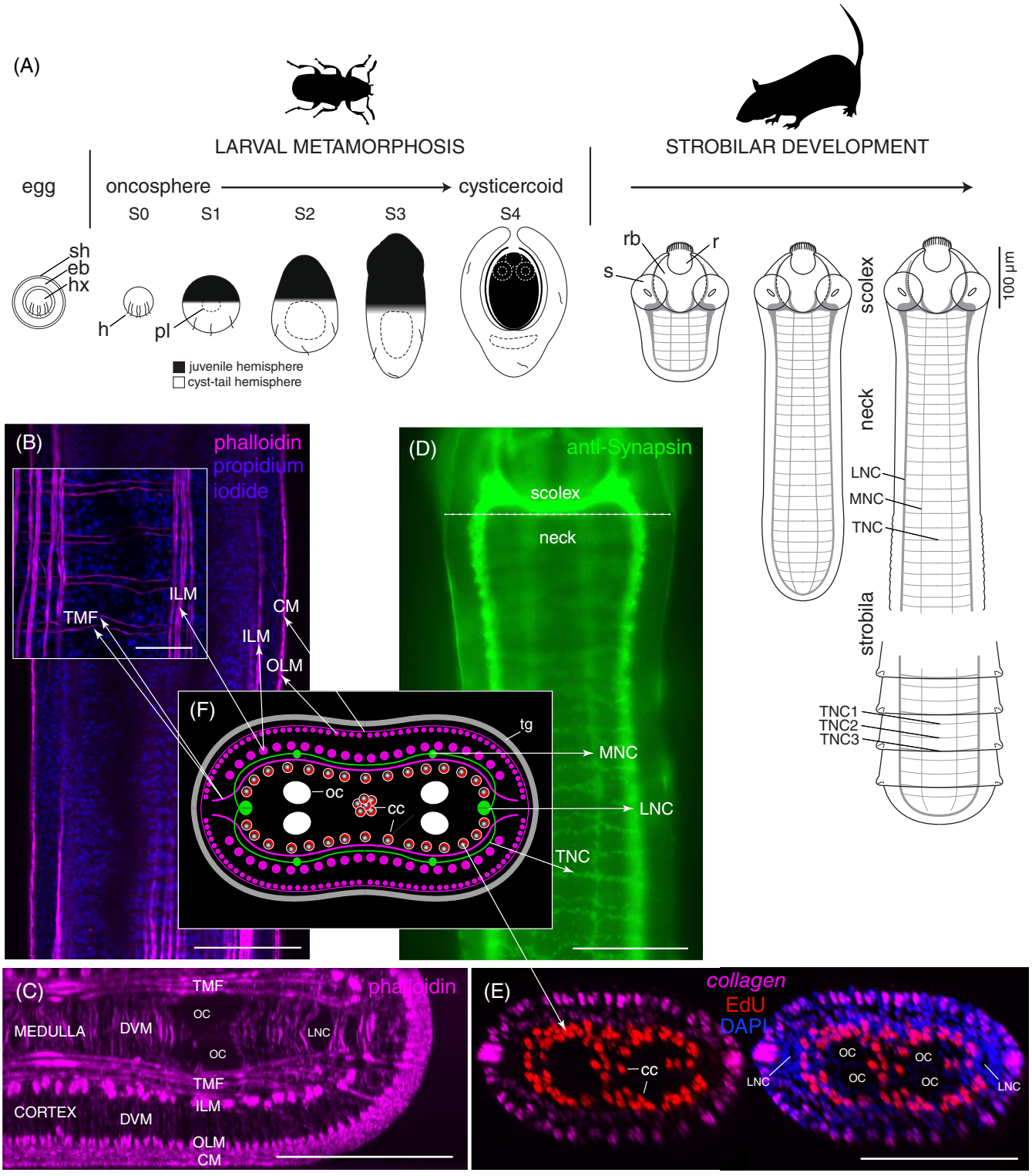

FIGURE 1 Legend on next page.

2 | RESULTS

2.1 | The internal body wall musculature shows evidence of early segmental patterning

Given the known expression of PCGs by muscle cells in planarians[15] and larval tapeworms,[5] we investigated the architecture of the musculature of adult *H. microstoma* (Figure 2). Unlike other segmented organisms, most of the musculature of tapeworms is not segmentally organized and consists instead of elements that run uninterrupted through the body.[4] Their musculature includes a sub-tegumental layer comprised of fine, outer circular (CM; Figure 2C) and thin longitudinal (OLM; Figure 2D) muscle fibers, an inner layer of thick longitudinal bundles of fibers (ILM; Figure 2F) that attach to the base of the rostellum (and by convention define the cortical-medullary boundary), and a dense array of fine, dorsoventrally oriented fibers that run through the parenchyma of the worm, except where interrupted by the osmoregulatory canals and reproductive elements (Figure 1C; Figure 2E,H).

At segmental boundaries there are dorsoventrally (DV) and AP-paired strands of transverse muscle fibers (TMFs) positioned inside the ILM layer (Figure 1B,C; see also[30]). These TMFs extend through the medullary region on either side of the main nerve cords into the cortex, where they attach (Figure 1C). Here, we trace their initial development to the start of the neck where they are first seen as fine, paired strands closely arrayed along the AP axis (Figure 2G). As the neck enlarges and transitions to the strobila they become progressively separated and come to define segmental boundaries (Figure 2I,J). To the best of our knowledge, these are the only muscular elements arranged in a segmentary distribution along the AP axis and are one of the earliest indications of segmentation during adult development, suggesting that muscle cells could participate directly in the segmentation process or that their precursors could be among the earliest cells to respond to signals regulating segmentation. In contrast, the major elements of the peripheral nervous system (PNS), which includes the main longitudinal (LNC), medial longitudinal (MNC), and transverse nerve cords, exhibit a flatworm-typical orthogonal pattern[31] (Figure 1D) that remains distinctly independent of the underlying segmentary pattern of the musculature until new, intra-segmental elements of the PNS form in maturing segments, discussed below. A recent study of peptidergic signaling in *H. microstoma* also shows the non-segmentary pattern of the nervous system in this region, evident from the positions of nerve cells along the LNCs and MNCs.[32]

2.2 | Spatial distribution of myocytons indicates their participation in PCG expression

The nuclei of flatworm muscle cells are contained in cell bodies called myocytons that are offset from the contractile part of the muscle cells (i.e., the muscle fibers) to

FIGURE 1 Life cycle, neuromuscular anatomy and cycling cells of the mouse bile-duct tapeworm *Hymenolepis microstoma*. (A) Major stages of larval metamorphosis and strobilar development (n.b. illustrations drawn to scale save the strobila detail; larvae staged according to Montagne et al.[28]). The life cycle is perpetuated when eggs expelled with mouse feces are consumed by grain beetles (e.g., *Tenebrio* spp.) releasing oncospheres that use their hooks to penetrate the intestine and enter the hemocoel where they metamorphose into encysted, juvenile worms called cysticercoids. Strobilar/sexual development commences when infected beetles are ingested by mice, releasing larvae that excyst in the stomach and slough their cyst tissues before entering the small intestine. There they undergo elongation of the body to form a neck region that generates the segmented strobila before the worms locate permanently in the bile duct. After around 2 weeks, the worms reach their maximum size and possess ~650 segments.[20] (B) Confocal imaging of the neck region of phalloidin stained worms shows the major muscle layers and AP-paired, transverse muscle fibers (TMF; inset) at segmental boundaries. (C) Transverse reconstruction at an early segment boundary shows that the TMFs are positioned inside the inner longitudinal muscle (ILM) layer and extend through the cortical region at the margins. Also visible is the array of dorsoventrally oriented muscle (DVM) fibers that run through the parenchyma, gaps in which show the positions of the osmoregulatory canals (oc) and main longitudinal nerve cords (LNC). (D) Fluorescent microscopy of anti-Synapsin staining shows the major elements of the nervous system in the scolex and neck, consisting of the main longitudinal (LNC), medial longitudinal (MNC) and transverse (TNC) nerve cords. Panel (E) and Additional files 1–3 show in vitro EdU labeling of cycling cells in the neck region (see Methods). Populations of these proliferative, neoblast-like somatic stem cells, called germinal cells, are located at the periphery of the medullary region and in the central region where the genital primordia develop. Also seen is expression of *collagen* by muscle cells representing the major muscle layers of the cortex (see Figure 4). (F) Diagram of the neuromuscular anatomy and cycling cells in the neck. cc, cycling cells; CM, circular muscle layer; eb, embryophore; h, hook; hx, hexacanth (= oncosphere) larva; ILM, inner, thick longitudinal muscle layer; oc, osmoregulatory canal; OLM, outer, thin longitudinal muscle layer; pl, primary lacuna (= cavity); r, hooked rostellum; rb, rostellar bulb; s, sucker; sh, membranous shell; tg, syncytial tegument; TMF, segmentally distributed transverse muscle fibers. All scale bars = 100 μm except C = 50 μm.

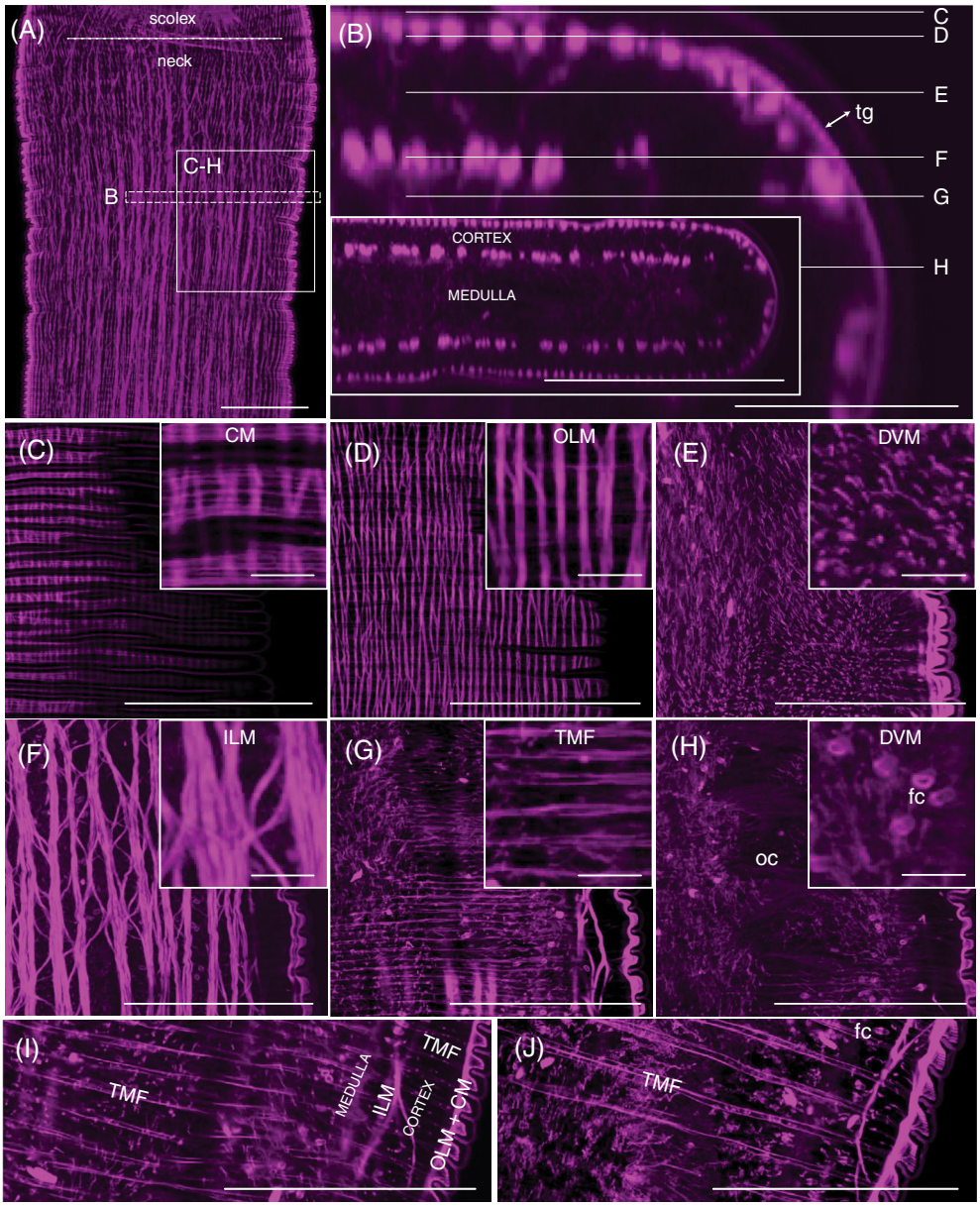

FIGURE 2 Phalloidin staining of the muscular system reveals early segmental elements formed in the neck. Standard deviation projection of the anterior neck region (A) shows locations of the transverse reconstruction in (B) and magnified areas in (C-H). B shows the focal planes of images C-H. Beneath the syncytial tegument (tg) is a layer of fine circular muscles (C) that are exterior and adjacent to the outer, thin longitudinal muscle layer (D) with which they are occasionally interwoven. The inner longitudinal muscle layer (F) has thick bundles of fibers and defines the boundary between the cortex and medulla (B inset). In both longitudinal muscle layers, the major strands are seen to form connections with neighboring strands (D, F). Immediately interior to the inner longitudinal muscle layer, we see the first indication of segmental patterning in the anterior of the neck with the development of AP-paired, transverse muscle strands that are closely arrayed along the AP axis (G). As the neck transitions to the strobila and segmentation of the body wall becomes visible they become further separated along the AP axis and come to define segmental boundaries (I, J). In the cortex (E) and medullary regions (H) are densely packed fine fibers that traverse the worm dorsoventrally (DV fibers), except where interrupted by the osmoregulatory canals (H) and genital primordia (not visible). CM, circular muscle layer; DVM, dorsoventral muscle fibers; fc, flame cell; ILM, inner longitudinal muscle layer; oc, osmoregulatory canal; OLM, outer longitudinal muscle layer; tg, syncytial tegument. Scale bars in A and C–J = 100 μm; 25 μm in B (inset in B scale bar = 100 μm); and inset scale bars in C–H = 10 μm.

which they are connected via thin cytoplasmic processes.[15] We visualized the spatial distribution of myocytons in adult worms by WMISH using probes for two muscular tropomyosin isoforms (*hm-tpm1*, HmN_000188900.3; *hm-tpm2*, HmN_000471300.3)[33,34] as well as an isoform of collagen (*hm-collagen*,

HmN_000398500).[15] No difference in pattern was discernible between the two isoforms of tropomyosin (cf. Figure 3A–D and Additional file 4). We identified several different myocyte populations according to their spatial distributions. In the cortex we identified myocytons associated with the CM and OLM layers immediately beneath the tegument (cortical myocytons; Figure 3B); myocytons associated with the ILM layer (Figure 3C); and uniquely clustered myocytons external to the LNCs that form ribbons along the lateral margins of the worm, hereafter referred to as "marginal myocytons" (arrows in Figure 3D–G). These clusters are paired by smaller foci of expression on the opposite (medullary) sides of the main nerve cords (arrowheads in Figure 3F,G). In the center of the medullary region is another prominent domain of expression (double arrowhead in Figure 3E–G) representing muscle cells that are likely intercalated between cells that contribute to the formation of the genital primordia, the precursors to the hermaphroditic proglottids.[35,36] Unexpectedly, we found that although the ILMs run continuously through the strobila, some of their myocytons become segmentally distributed along the AP axis in maturing segments (Figure 3H), resulting in three "stripes" that correspond spatially to the three transverse nerve cords that form in each segment (Figure 3I).[4,30] The spatial arrangement of these myocytons thus points to concerted development between the musculature and segmental patterning of the PNS.

We also investigated the spatial patterns of myocytons via expression of *collagen* (Figure 4; Additional file 2) as muscle cells have been shown to be the main cell type expressing diverse extracellular matrix components in the parenchyma of planarians.[37] *Hm-collagen* was found to be expressed in a more restricted set of myocyton populations than *tpm1/2*, with little expression seen in the scolex (Figure 4A) and medullary regions (Figure 4B). Strong expression was seen in the cortical region, including the marginal myocytons (Figure 4B–D), and transverse reconstructions show circumferential expression (Figure 4B,F,G) associated with the outer and inner muscle layers.

We also examined *collagen* expression during larval metamorphosis and found it to be restricted to the posterior hemisphere of the larva, forming a wide band that marks the region of the developing cyst tissues (Figure 4H–J). Similar to expression in adults, *collagen* is restricted to a subset of the total larval muscle cell population as recently described by Montagne et al.[38] However, these results corroborate previous findings of the massive production of collagen by muscles in the cyst tissue of *H. microstoma* larvae, resulting in the deposition of three layers of collagen strands that protect the encysted juvenile from mechanical injury.[39]

Most of the broader patterns of expression in myocyton populations revealed by *tpm1/2* and *collagen* can be clearly associated with the different major elements of the musculature (e.g., cortical myocytons are associated with the cortical muscle fibers Figure 2). However, independent visualization of the nuclear and contractile bodies of the myocytes prevents us from being able to make definitive assignments between individual myocytons and their corresponding muscle fibers.

2.3 | Wnt inhibitors are expressed in the scolex and neck

We found that the scolex and neck are characterized by the expression of secreted frizzled receptor (sFRP) genes (Figure 5) which are inhibitors of Wnt signaling.[12] Tapeworms have two sFRP genes: a homolog of sFRPs that canonically act to specify the anterior pole in metazoans (*hm-sfrp*; HmN_000556500) and a *sfrp*-like paralog (*hm-sfl*; HmN_000359400) with a divergent netrin domain, both of which were found to be expressed in anterior domains in larval worms.[5] In adult worms, *sfrp* is expressed in the scolex and neck before being abruptly downregulated at the start of the strobila where segmentation of the body wall first becomes visible (Figure 5A). Its expression in the neck is seen in the outer cortex (Figure 5B), and in the marginal myocytons, including the associated medullary foci (arrows/arrowheads in Figure 5C,F). A number of internal foci are also seen in the scolex and confocal reconstruction of *sfrp* together with anti-Synapsin staining[30] shows that they are associated with the cerebral ganglia and terminal branches of the CNS that innervate the holdfast structures (Figure 5D,E).

Hm-sfl is also expressed in the scolex and neck region but differs from the pattern of *sfrp* in most other respects (Figure 6). In particular, it is also expressed segmentally and thus in all regions of the adult worm (Figure 6A), exhibiting the most comprehensive set of expression domains of the components investigated. In the neck region (Figure 6B–F), its expression further differs from *sfrp* in being expressed in medullary domains and not in the cortex, save the marginal myocytons in which both inhibitors are expressed. At the DV boundary (Figure 6C) *sfl* shows expression in the marginal myocytons and associated foci, as well as in the central region, mirroring the muscular expression pattern of *tpm1* (Figure 3F,G). Additional foci are seen that are semi-regularly spaced along the AP axis on the dorsal and ventral sides of the LNC (Figure 6D), and at the cortical-medullary boundary there are neural-related foci that follow the pattern of the

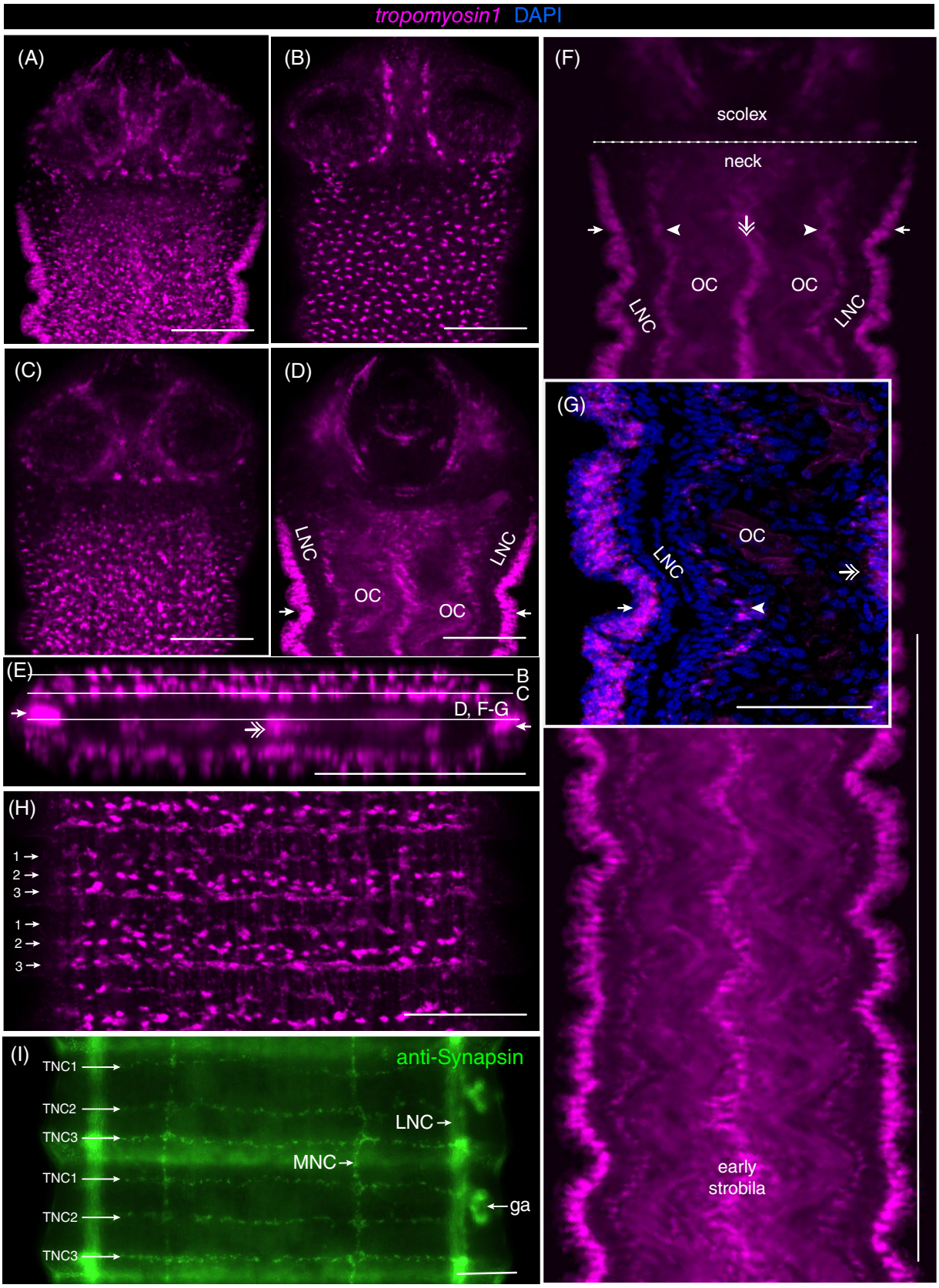

FIGURE 3 Legend on next page.

MNCs (Figure 6E), and which are also foci of *hedgehog* expression, discussed later.

2.4 | Strobilar development involves AP-polarized expression of Wnt inhibitors and ligands

In the transition from the neck to strobila, we observe a change in patterning of *sfl* and the first instances of AP-polarized expression of inhibitors and wnts (Figure 7). In this region, new dorsal and ventral pairs of *sfl* + foci originate along the cortical-medullary boundary, forming an expression pattern hereafter referred to as the "signaling quartet" (SQ). These new domains arise in register with the early segmentation of the body wall and are initially positioned close together near the midline. As the nascent strobila develops the paired foci are observed to widen laterally toward the position of the MNCs, and in the transition to the strobila *sfl* expression in the SQ diminishes at the same time as new, midline foci of expression appear (Figure 7A, Additional file 5).

The appearance of the *sfl* + SQ precedes the first instance of posterior Wnt gene expression during strobilar growth (Figure 7B). Expression of *hm-wnt1* (HmN_000328000), a homolog of the Wingless/Int gene family, begins later in the SQ (Figure 7B–D) and double fluorescent in situ hybridization (FISH) shows that it initially co-localizes with *sfl* in these foci (Figure 7G–I). As *wnt1* expression in the SQ increases, *sfl* diminishes and a new midline foci of expression appears at the cortical-medullary boundary, in between the paired foci of the SQ (Figure 7D, Additional file 6). In the transition to the early strobila, the foci of the SQ widen toward the positions of the MNCs (Figure 7J–M) and come to register with segment boundaries (Figure 7C,D,H).

In the strobila, the *sfl* expression domains that begin in the neck and transition zone become segmental and AP-polarized with *wnt1* expression (Figure 8, Additional file 7). As segments mature new circumferential expression domains of both *sfl* and *wnt1* in the cortical region appear, marking the segments with AP axes in agreement with the polarity of the main body axis (Figure 8A,C,F). Although expression in the SQ may persist throughout strobilar development, the distinct quartet pattern quickly becomes confounded by additional sites of expression (cf. Figure 8B,D). *Wnt1* expression is notably absent from the marginal myocytons (Figure 8B,E,H) whereas *sfl* expression in these domains is strong in the anterior of the segments and diminishes posteriorly along the LNCs (Figure 8C,F). At segmental boundaries *sfl* is also expressed in a line of foci that traverses the DV boundary (Figure 8D,G).

2.5 | Expression of *wnt11a* demarcates the transition to strobilar development

The transition between the neck and strobila forms a morphological gradient marked by out-pocketing of the outer body wall. Strikingly, this region is tightly demarcated by the expression domain of one of two Wnt11 paralogs (*hm-wnt11a*; HmN_002147900) that starts prior to and includes the first visible signs of segment formation (Figure 9, Additional file 8). Upregulation of *wnt11a* in this zone begins in the marginal myocytons and central region and is then expressed circumferentially in the cortical region (Figure 9D–F). Double FISH shows that expression begins in register with *wnt1* and then fades as *wnt1* expression increases and becomes expressed circumferentially (Figure 9F). Expression of *wnt11a* is thus highly ephemeral and demarcates a transition zone along the AP axis roughly equal in length to that of the neck (~500 um). Results also show that it is expressed in cell populations distinct from those that are *wnt1*+ and that are positioned just above (anterior) to the *wnt1* domains (Figure 9D). The onset of *wnt11a* expression is also shown to coincide with appearance of *sfl* expression in the SQ (Figure 9G). In the central region, *wnt11a* expression begins and fades earlier in development than in the

FIGURE 3 *Tropomyosin* expression shows the spatial distribution of muscle cell nuclei. Expression of *hm-tpm1* shows the punctate pattern of myocytons in the different muscle layers and regions of the body. Panel A shows a maximum projection of the scolex and anterior neck and B–D show single focal planes corresponding to the outer and inner muscle layers and DV boundary, as indicated in the transverse reconstruction in (E). F shows an image through the DV boundary of the scolex, neck and early strobila, and the inset (G) shows higher magnification at the neck margin. Clusters of myocytons (arrows), referred to as marginal myocytons, and their opposing, internal foci (arrowheads) are seen arrayed along the main longitudinal nerve cords, forming prominent ribbons of expression along the margins of the worm. Myocytons are also arrayed down the center of the worm (F, double arrow) where groups of cells give rise to the genital primordia. In the early strobila, the pattern becomes noticeably segmental with gaps in signal becoming visible between foci (F). In more mature segments, myocyton populations are seen arrayed along the AP axis in transverse rows (H) that correspond to the positions of the three transverse nerve cords (TNC1-3) that develop in each segment (I). Also visible are nervous elements associated with the genital atria (ga) where the male and female ducts open at the dextral margin. LNC, main longitudinal nerve cord; MNC, medial longitudinal nerve cord; oc, osmoregulatory canal. All scale bars = 100 μm except F = 500 μm and G = 50 μm.

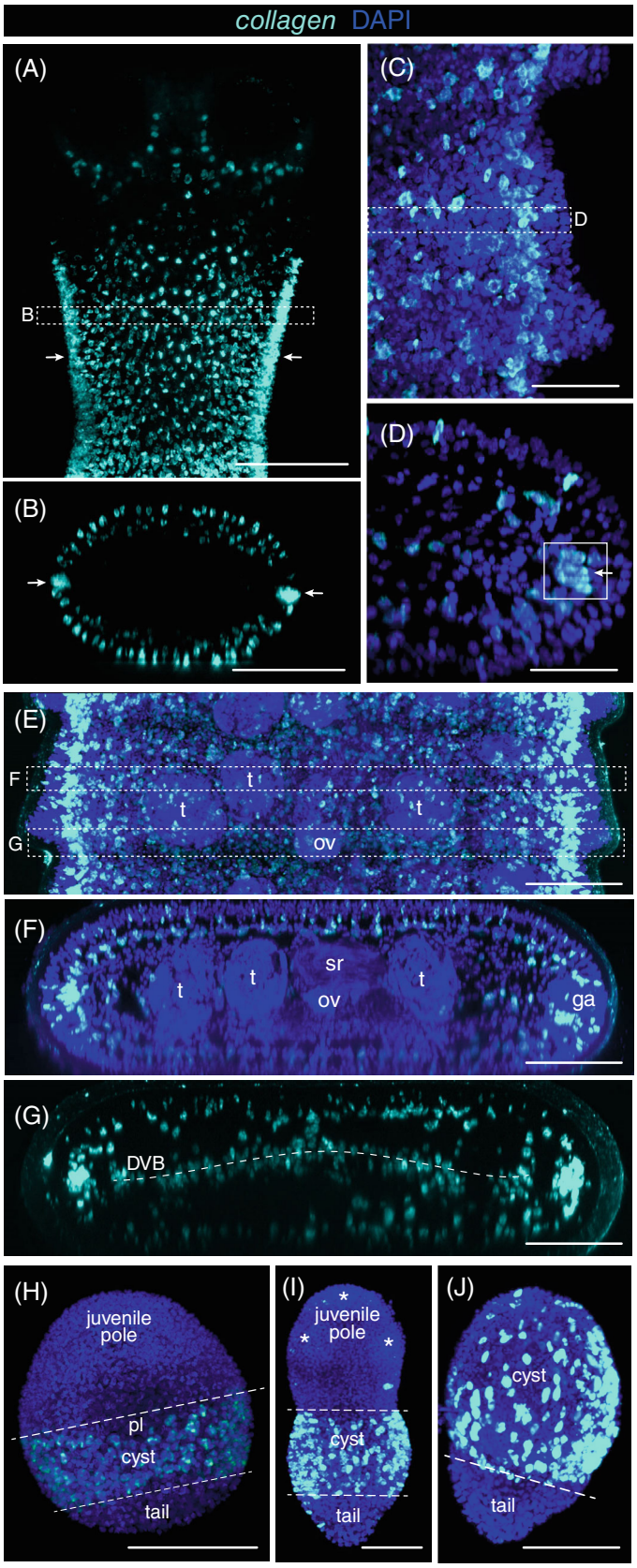

FIGURE 4 Legend on next page.

cortical tissues, giving the appearance of an anteriorly offset streak (Figure 9G, Additional file 8).

2.6 | *Wnt11b* and *notum* expression is restricted to the strobila

Expression of the other Wnt11 paralog, *hm-wnt11b* (HmN_000022800), is similar in pattern to *wnt1* but starts abruptly in the strobila rather than being upregulated gradually in the transition zone (Figure 10). Like *wnt1*, *wnt11b* is restricted to the posterior segmental boundaries and becomes circumferential as segments mature, but differs in also being expressed in the marginal myocytons and in a line across the DV boundary at the limit between segments (Figure 10E,G), similar to *sfl* expression (cf. Figure 8G) with which it is AP-polarized. Posterior segmental boundaries in the strobila are thus marked by expression of the posterior Wnt genes *wnt1* and *wnt11b*.

Like sFRPs, Notum is an inhibitor of canonical Wnt signaling[40] and is widely involved in neurogenesis.[41] In planarians, Notum is required for respecification of the anterior pole[42,43] and brain development during regeneration.[44] *Hm-notum* (HmN_000848900) expression (Figure 10H–L) was observed in a small number of foci in the scolex (Figure 10I) but was otherwise restricted to four foci associated with the positions of the MNCs at segment boundaries that we suggest represents the SQ pattern (Figure 10J,K). Like *wnt11b*, *notum* expression starts abruptly in the strobila after the initial formation of segments in the transition zone. As it was not included in our previous investigations,[5] we investigated *notum* expression in larvae and found that it is expressed in two subapical foci at the anterior pole (Figure 10L).

2.7 | Frizzled receptor genes show regionalized expression in domains that mirror *sfl*

Proteins of the Frizzled family function as surface receptors of secreted Wnt ligands and may also be bound by inhibitors which block ligand binding. Like other Wnt signaling components they typically have distinct expression domains along the AP axis during embryogenesis.[45] We examined the expression of three frizzled genes with predicted roles in Wnt signaling: *hm-fzd5/8* (HmN_000386300), *hm-fzd1/2/3/6/7* (HmN_000227100) and *hm-fzd4* (HmN_000319700). Strikingly, in the neck and transition zone these genes showed expression in most of the domains that express *sfl*, but differed in the strength of expression regionally along the AP axis (Figure 11). Homologs of *fzd5/8* have a canonical role in specifying the anterior pole and are expressed in the anterior organizer of adult planarians.[46] We found weak expression of *hm-fzd5/8* at the base of the rostellum followed by very gradual upregulation of expression in the neck in the marginal myocytons (arrows Figure 11A,H,K) and in medullary expression domains internal to the LNC (arrowheads) and in the central region (double arrow). It is also expressed in the SQ in the transition zone (Figure 11B). These patterns mirror those of *sfl*, with the exceptions of domains of *sfl* expression associated to the nervous system (the DV-paired foci along the LNCs [Figure 6D] and MNC-related foci [Figure 6E]). In the strobila, *fzd5/8* is also expressed at the anterior of the segments like *sfl*, and eventually becomes circumferential (Figure 11C–F). Also like *sfl* it shows diminishing expression in the marginal myocytons posteriorly (Figure 11E) and in foci that traverse the DV boundary in between the segments (Figure 11F).

Fzd1/2/3/6/7 expression begins abruptly in the anterior of the neck where the marginal myocytons first appear along the AP axis (Figure 11H) and also shows punctate expression in the cortical tissues (Figure 11G) and in the early SQ. Its expression is significantly downregulated but not extinguished in the early strobila (Figure 11I), and an identical pattern was described by Rozario et al.[47] for the ortholog in *H. diminuta* (HDID_0000773501) that was identified in an RNA-Seq screen for genes enriched in the anterior of the neck.

Fzd4 expression (Figure 11J,K) begins gradually in the neck similar to *fzd5/8*, and in maturing segments also shows diminishing expression in the marginal myocytons, as well as taking on a more general pattern of punctate expression throughout the body (Figure 11L) which

FIGURE 4 *Collagen* shows expression domains in muscle cells. *Hm-collagen* expression is seen in a more restricted set of myocyton populations than seen in *hm-tpm1/2* (cf. Figure 3/Additional file 4) and is primarily cortical. In the scolex (A), there are few *collagen* + cells, whereas the punctate pattern of the main muscle layers, together with the clustered pattern of the marginal myocytons (arrows), is seen throughout the neck (A, B) and strobila (E–G). Higher magnification at segment margins (C, D) shows the clustered arrangement of the marginal myocytons (box in D). Punctate expression corresponding to the muscles layers is evident in mature segments, and at segmental boundaries (G) a line of medullary foci is seen along the dorsoventral boundary (DVB; dashed line). During larval metamorphosis *collagen* is expressed in the cyst tissues that develop in the posterior hemisphere (H, I) and eventually encyst the nascent worm (J).[5] Asterisks in I show condensations of cells around the positions of the holdfast structures of the scolex which develop post-encystment.[38] ga, genital atrium; ov, ovary; pl, primary lacuna; sr, seminal receptacle t, testis. Scale bars in A, B and E–G = 100 μm; 50 μm in C, D and H–J.

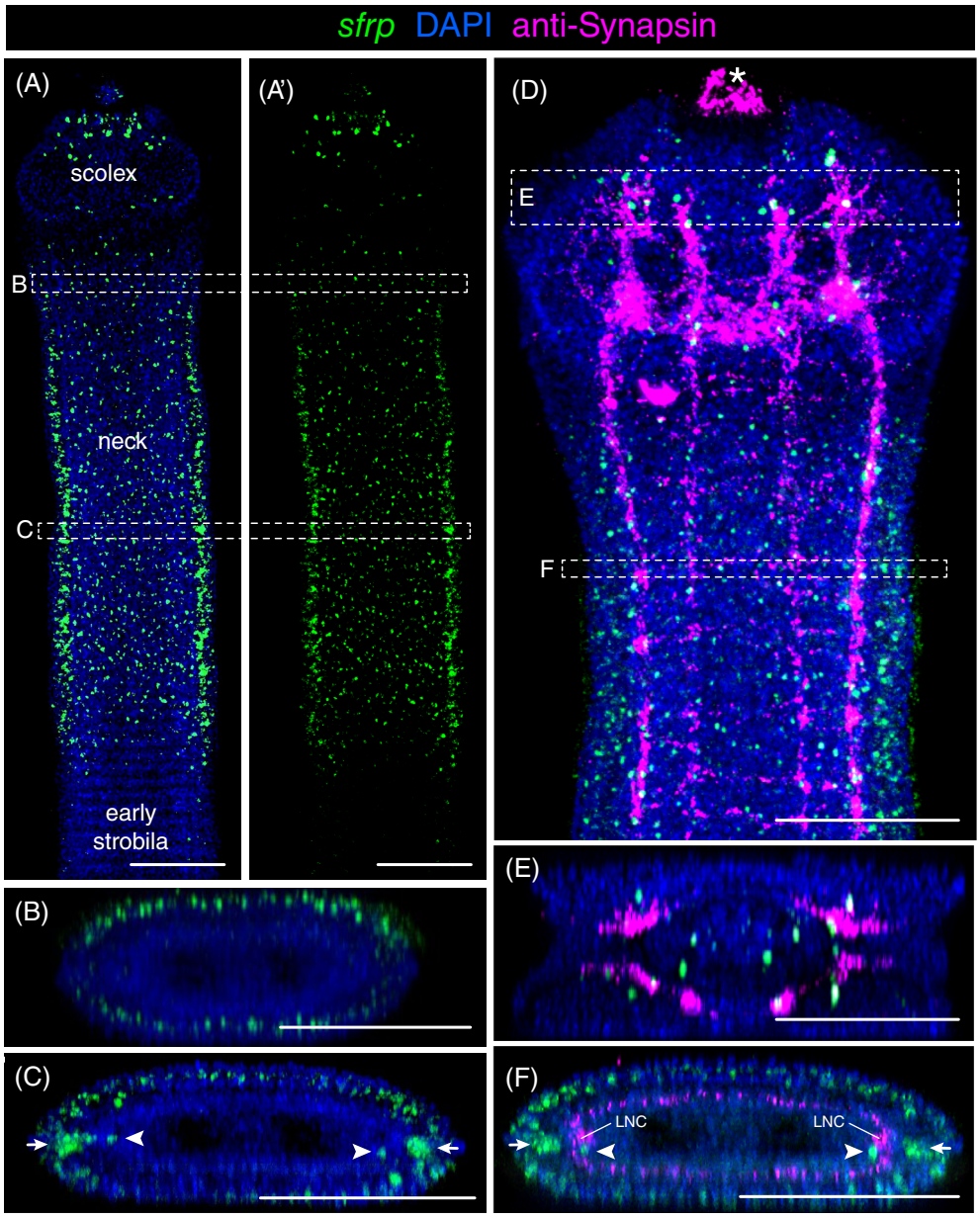

FIGURE 5 Expression of *sfrp* marks the scolex and neck as Wnt inhibitory. Expression of *hm-sfrp* is restricted to the scolex and neck region and is abruptly downregulated at the start of the strobila (A). Transverse reconstructions show that expression in the neck is restricted to the outer cortex (B), while in the posterior neck region there is also expression in the marginal myocytons (arrows) and internal, accompanying foci (arrowheads) associated with the main longitudinal nerve cords (LNC) (C). Combined with anti-Synapsin staining shows that expression in the scolex is associated with the major elements of the central nervous system (D, E), whereas reconstruction through the neck region (F) confirms that expression is restricted to the outer muscular layers and marginal myocytons. Asterisk in panel D indicates artifactual signal in the glandular, rostellar bulb (see also[30]). Scale bars = 100 μm.

is seen in mature segments in all three frizzled genes. In regenerating planarians, *fzd4* is upregulated in posterior blastemas, suggesting a potential role in reorganizing the posterior pole.[5,48] In *H. microstoma*, it is expressed in the anterior of the body, the neck, and in the strobila appears strongest in the anterior of the marginal myocytons within segments. However, it does not become expressed circumferentially at the anterior of the segments like *fzd5/8* and *sfl*, and punctate expression foci in the body do not exhibit any kind of AP pattern (Figure 11L). Thus, whereas *hm-fzd4* shows posterior expression during larval metamorphosis,[5] similar to planarian regeneration, during adult development segmental expression domains do not appear strongly AP-polarized.

2.8 | *Hedgehog* is expressed with *sfl* in neural-related domains

Hedgehog signaling has been shown to be an upstream promotor of Wnt signaling in flatworms[49] and we investigated *hedgehog* expression in larval and adult worms (Figure 12). Combined with anti-Synapsin staining shows that *hm-hedgehog* (HmN_000068600) is expressed in the scolex in foci associated with the CNS (Figure 12A). In the neck, it is expressed at the junctions of the medial and transverse nerve cords (Figure 12B) and in clusters of cells in the central region, and both domains persist into the strobila. Double FISH shows that *hedgehog* co-localizes with *sfl* in both the nerve junctions (boxes in Figure 12D,D″) and central region (Figure 12E,E″).

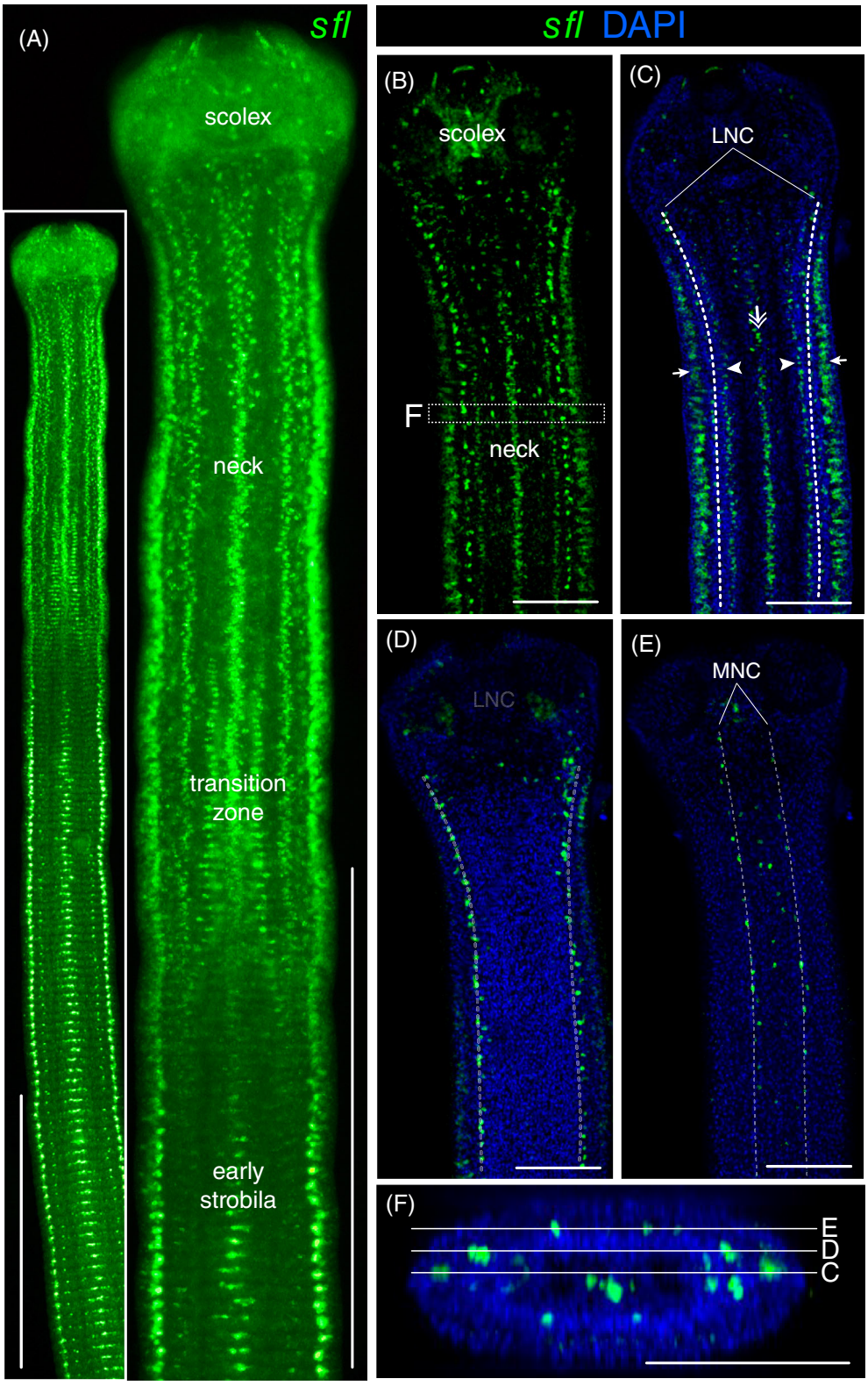

FIGURE 6 The *sfrp* paralog *sfl* is expressed in the scolex and neck and segmentally in the strobila. Fluorescent micrographs show dynamic expression of the inhibitor *hm-sfl* along the AP axis (A). B–F show confocal micrographs of *sfl* in the scolex and neck region, up to the transition zone described in Figure 7. B shows a maximum projection and C–E show single focal planes at the levels indicated in the transverse reconstruction (F). In the scolex, there are few foci (B) that appear more cortical than the CNS-associated domains of *sfrp* (Figure 5D,E). At the dorsoventral boundary (C), *sfl* is expressed in the marginal myocytons (arrows) and internal, associated foci (arrowheads) associated with the main nerve cords (LNC), as well as in the central region (double arrows), mirroring the muscular expression domains of *tpm1* at the dorsoventral boundary (Figure 3). Additional foci are also seen along the dorsal and ventral sides of the LNC (D) and at the cortical-medullary boundary (E), there are foci that follow the pattern of the medial longitudinal nerve cords (MNC; Figure 1D), and in which *sfl* co-localizes with *hedgehog* expression (see Figure 12D). Scale bars = 500 μm in A; 100 μm in B–F.

In the transition zone and early strobila, *hedgehog*/*sfl* expression in the nerve junctions follows the orthogonal pattern of the nervous system, which remains independent of the segmental pattern as represented by the start of *sfl* expression in the SQ (Figure 12D′,D″). However, in the transition to the strobila, the SQ pattern shifts to the positions of the MNCs along the cortical-medullary boundary, at which point neural-related expression of *hedgehog*/*sfl* becomes spatially associated with these domains. During larval development, *hedgehog*

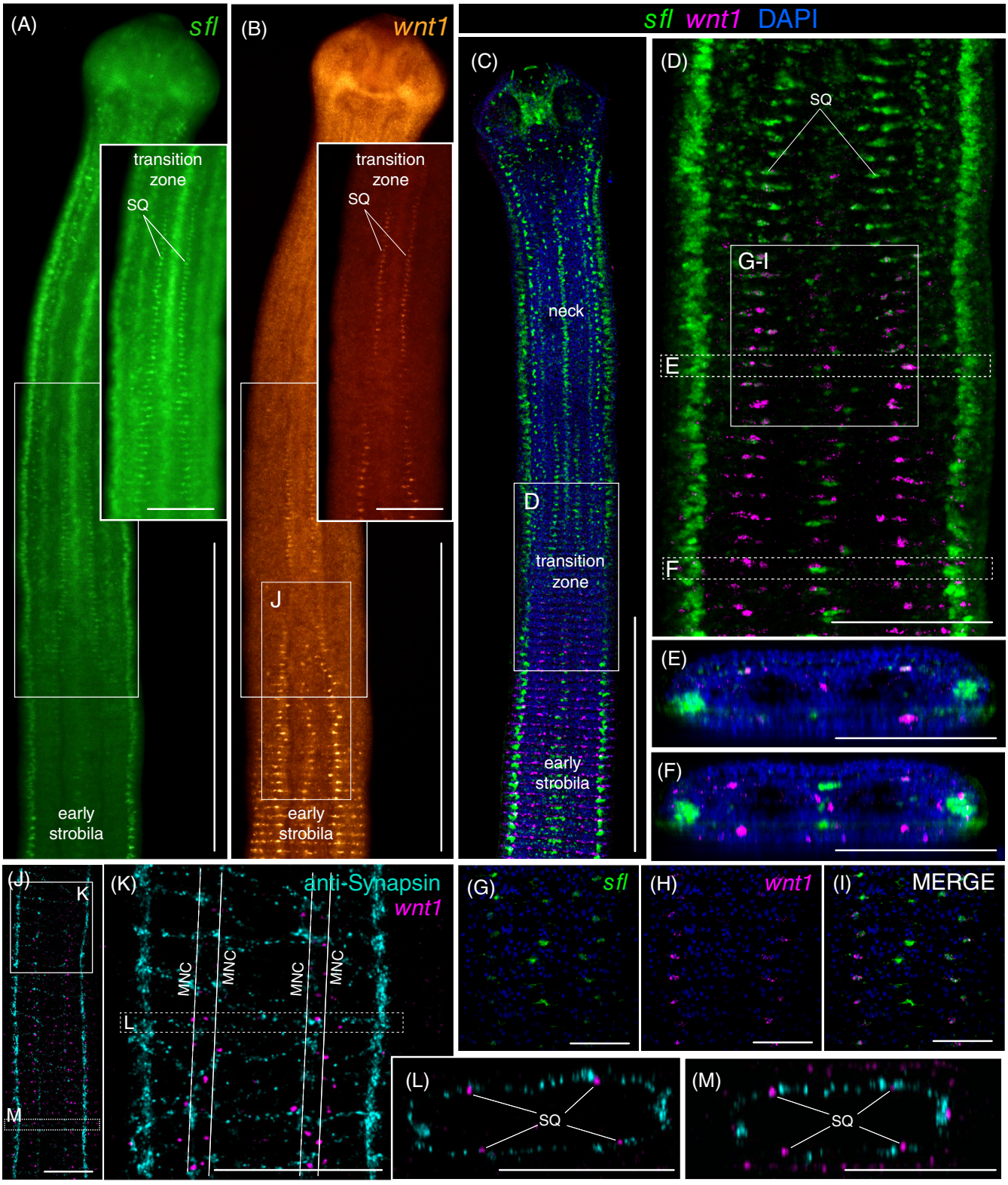

FIGURE 7 Initial expression of the canonical posterior gene *wnt1* shows co-localization with the inhibitor *sfl*. Fluorescent micrographs show that in the transition from the neck to strobila four new prominent, paired foci of *sfl* appear in a segmentary pattern near the midline of the worm (A, for 3D reconstruction see Additional file 5). These foci are referred to as the signaling quartet (SQ) and it is in these cells that we observe the first instance of posterior wnt expression during adult development (B, C). Confocal imaging (C–I) shows that *hm-wnt1* first becomes upregulated in *sfl* + cells in the SQ (G–I) and that its expression in these foci increases into the strobila at the same time as expression of *sfl* decreases (for 3D reconstruction see Additional file 6). In this transition zone, the paired foci become separated laterally (B) and a new focus of expression is seen at the midline (B). Specimens co-stained with anti-Synapsin (J–M) show that in the nascent strobila the SQ pattern becomes spatially associated with the positions of the medial longitudinal nerve cords (MNC). Scale bars in A–C = 500 μm; 100 μm in D–F and J–M; and 10 μm in G–I.

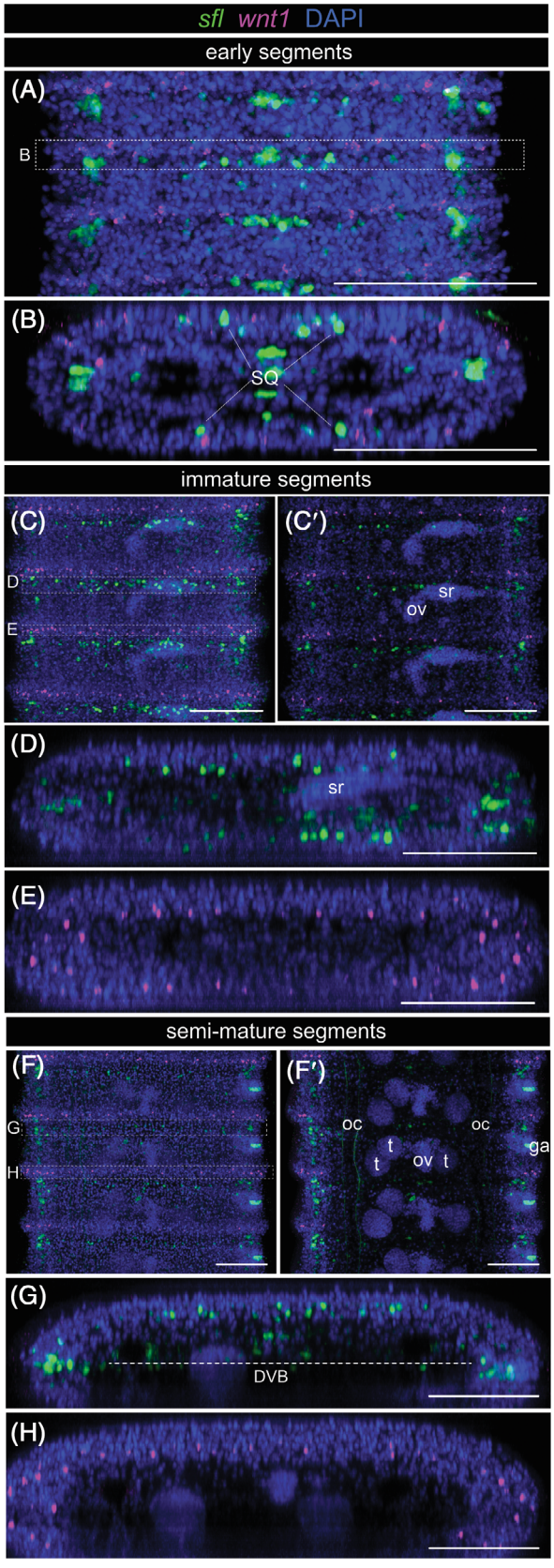

expression (Figure 12F–I) marks the sagittal midline on the dorsal and ventral surfaces of the hemisphere that gives rise to the juvenile worm, consistent with a canonical role in midline patterning,[50] and is juxtaposed with *sfl* expression along the L-R margins (Figure 12I).

3 | DISCUSSION

3.1 | Strobilar growth reveals domains of PCG expression associated with the neuromuscular system

The patterns revealed by *tropomyosin* and *collagen* encompass most of the expression domains of the Wnt ligands, inhibitors and receptors, consistent with Wnt signaling being established and maintained by the musculature.[15] Unexpectedly, expression of these muscle markers revealed the clustered arrangement of myocytons at the margins that run continuously through the neck and strobila and are thus not overtly segmental in their arrangement. However, PCG expression in these clusters becomes markedly discontinuous, segmental and AP-polarized. They are also positioned at the DV boundary which has been described as an organizing center in planarians[14] and other animals, and are immediately exterior to the main LNCs, allowing for close, cell–cell communication between the systems. We suggest that these uniquely arranged myocytons act as signaling centers, or organizers,[51] that regionalize the AP axis during adult growth. It is notable that clustered myocytons are not observed in planarians,[15] although a much broader

FIGURE 8 *Sfl* and *wnt1* expression is AP-polarized at segment boundaries. Early segments show AP-polarized expression of *sfl* and *wnt1* at segment boundaries (A), marking each segment with AP axes in agreement with the polarity of the main body axis (for 3D reconstruction see Additional file 7). Transverse reconstruction (B) showing the pattern of the signaling quartet (SQ). Expression in the SQ during later segment development becomes confounded by the presence of new foci that encircle the worm (C–H). *Sfl* expression in the marginal myocytons, which do not express *wnt1*, is strong in the anterior of the worm and is downregulated at the posterior of each segment (C, G). At segment boundaries *sfl* is also expressed in a line of medullary foci along the dorsoventral boundary (DVB; D, H; see also *collagen* expression, Figure 4F′,G). ga, genital atrium; oc, osmoregulatory canal; ov, ovary; sr, seminal receptacle; t, testis. Scale bars = 100 μm.

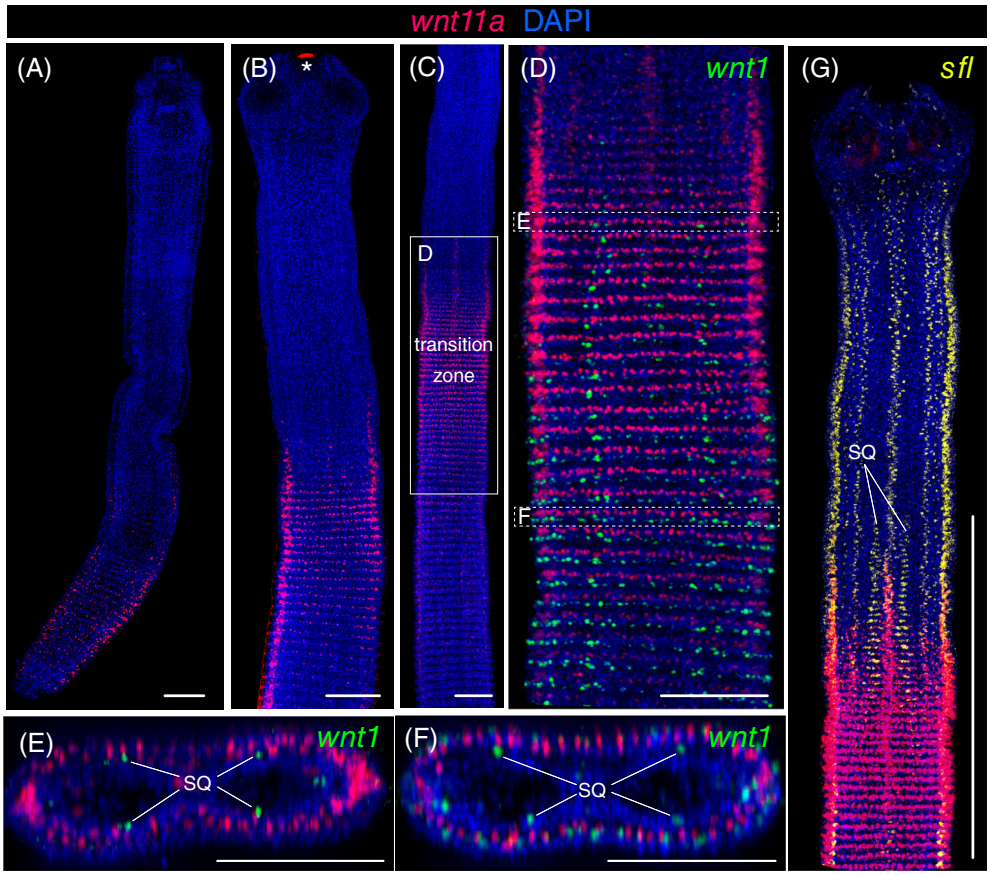

FIGURE 9 *Wnt11a* specifically marks a transition zone between neck and strobila. Expression of the posterior Wnt11 gene *hm-wnt11a* is tightly restricted to the transition zone between the neck and strobila where segmental signaling via AP-polarized expression of *sfl* and *wnt1* begins in the signaling quartet pattern (SQ, Figure 7). Its expression is shown in three-day-old, pre-strobilar juvenile worms (A) and in strobilar adults (B–D, see also Additional file 8 for 3D reconstruction). D shows detail of *wnt11a* along with the start of *wnt1* expression in the SQ. Transverse reconstructions show circumferential domains of *wnt11a* in the cortex, as well as expression in the marginal myocytons and in the central medullary region (E). Double FISH shows that the cortical domains *wnt11a* are separate from those of *wnt1* (D, F) and that *wnt11a* is upregulated just after the first appearance of *sfl* in the SQ (G; in this image expression in the central medullary region is also more apparent). Asterisk in B indicates artifactual signal in the rostellum. Scale bars in A–F = 100 μm; 500 μm in G.

survey of myocyton patterns in flatworms is needed to determine the extent to which this arrangement could be unique to tapeworms or to *H. microstoma*.

The structure of the AP-paired TMFs that develop in the neck could provide a means to produce polarized expression of PCGs at segment boundaries and thus account for expression in the *sfl*+/*wnt*1+ SQ. It is also possible that they could account for segmental discontinuity of expression in the marginal myocytons, as the TMFs extend past the LNC into the cortex (Figure 1C) and could contribute to segmentally arranged myocyton populations within the otherwise continuous arrays of marginal myocytons. However, we also find that myocytons in the otherwise continuous longitudinal muscles can come to be arranged segmentally (Figure 3H) which could instead account for discontinuous signaling in the marginal myocytons. Finally, being positioned at the cortical-medullary boundary, we cannot exclude the possibility of expression in germinative cells or their differentiating progeny. In any case, we suggest that the SQ also represents a signaling center for patterning the AP axis which is associated with the onset of strobilation and/or proglottization.

In planarians, Scimone et al.[16] and Witchley et al.[15] identified wnt ligands and frizzled receptors expressed by different subsets of musculature, suggesting signaling between muscle layers. Although we cannot definitively assign the expression of Wnt components to the different muscles, we suggest that concordance in the patterns of *tpm1* (Figure 3), *sfl* (Figures 6–8) and *fzd5/8* (Figure 11) points to modulation of Wnt signaling between muscle cells, which could be employed to maintain these foci as wnt inhibitory. Similarly, punctate expression of *fzd1/2/3/6/7* in the outer cortex (Figure 11G) could be associated with *sfrp* signaling in the neck, which in turn could have a role in preventing ectopic initiation of

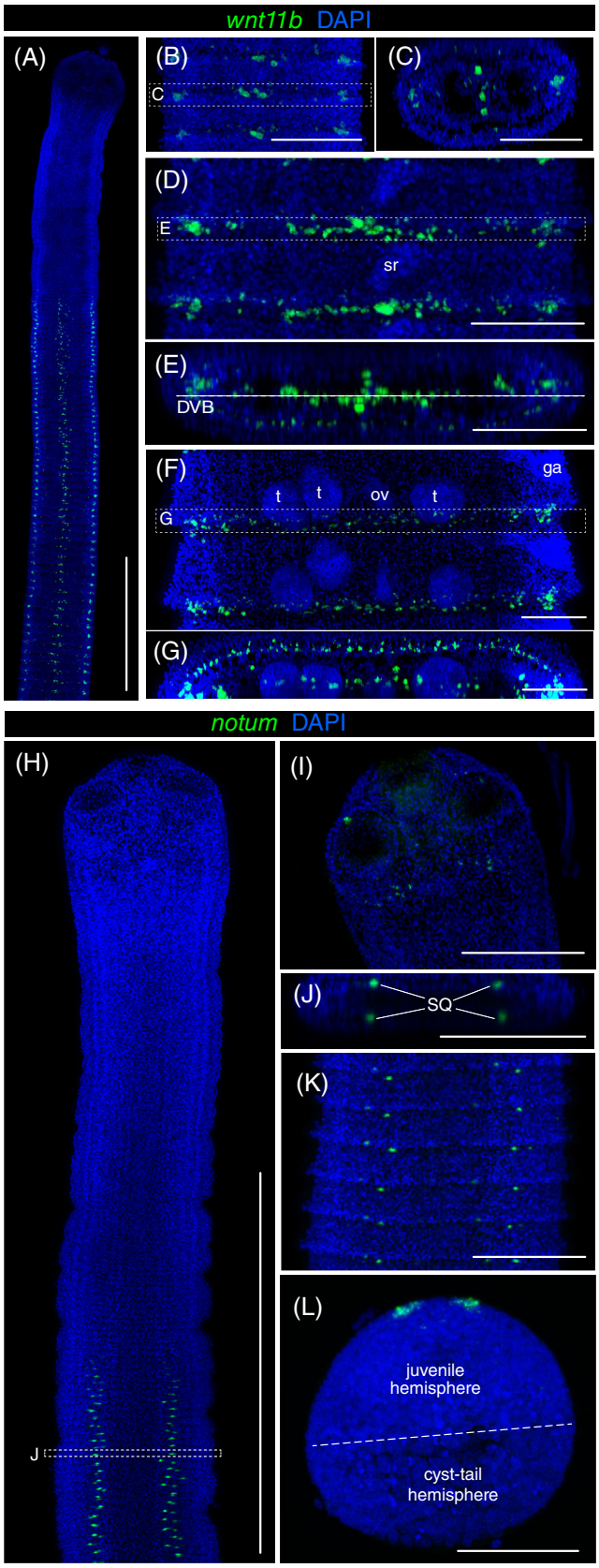

segmentation by marking the region as wnt inhibitory, thus maintaining an unsegmented region. Future testing of co-localization among these factors and Wnt components will help clarify these possibilities. Interestingly, Rozario et al.[47] demonstrated that anterior fragments of the neck region of *H. diminuta* have the ability to generate new proglottids in vitro, whereas very few proglottids were generated by middle and posterior fragments. Taking into account the results here, it is possible that in the posterior neck fragments only the transition zone that had already initiated segmentation was present, or that an unsegmented germinative region could not be stably maintained without signals elicited from the boundary between the neck and scolex.

3.2 | Wnt expression defines secondary segmental axes

The components of Wnt signaling are expressed along the AP axis in a highly regionalized pattern (Figure 13) with the scolex and neck characterized by expression of inhibitors, the transition zone by upregulation of posterior ligands and the strobila by AP-polarized expression of inhibitors and ligands. In tapeworms, these regions represent developmental periodicities that illustrate the dynamic changes in signaling, with *wnt11a* being an

FIGURE 10 *Wnt11b* and *notum* expression begins in the strobila. The posterior Wnt11 gene *hm-wnt11b* is expressed segmentally at the posterior margins and is upregulated abruptly in the strobila post-transition zone (A). Early segments (B) show expression in the marginal myocytons, in the central medullary region, and in DV foci at the midline of the cortical-medullary boundary (C). In maturing segments (D–G) expression becomes circumferential in the cortical region, and in a line of medullary foci (E, G) along the dorsoventral boundary (DVB), as seen in *collagen* (Figure 4G) and *sfl* (Figure 8G). Expression of the Wnt inhibitor *hm-notum* (H-L) is similarly restricted to segmental boundaries in the strobila (H) with the exception of a small number of foci in the scolex that are likely associated with the CNS (I). In the strobila it is expressed in four foci (J, K) near the positions of the medial longitudinal nerve cords that we suggest represent the pattern of the signaling quartet (SQ) (cf. Figure 7M). In stage 2 larvae (L) *notum* is expressed in bilaterally symmetrical, apical clusters of cells at the anterior pole. ga, genital atrium; ov, ovary; sr, seminal receptacle; t, testis. Scale bars in A and H = 500 μm; 100 μm in B-G and I-K; 50 μm in L.

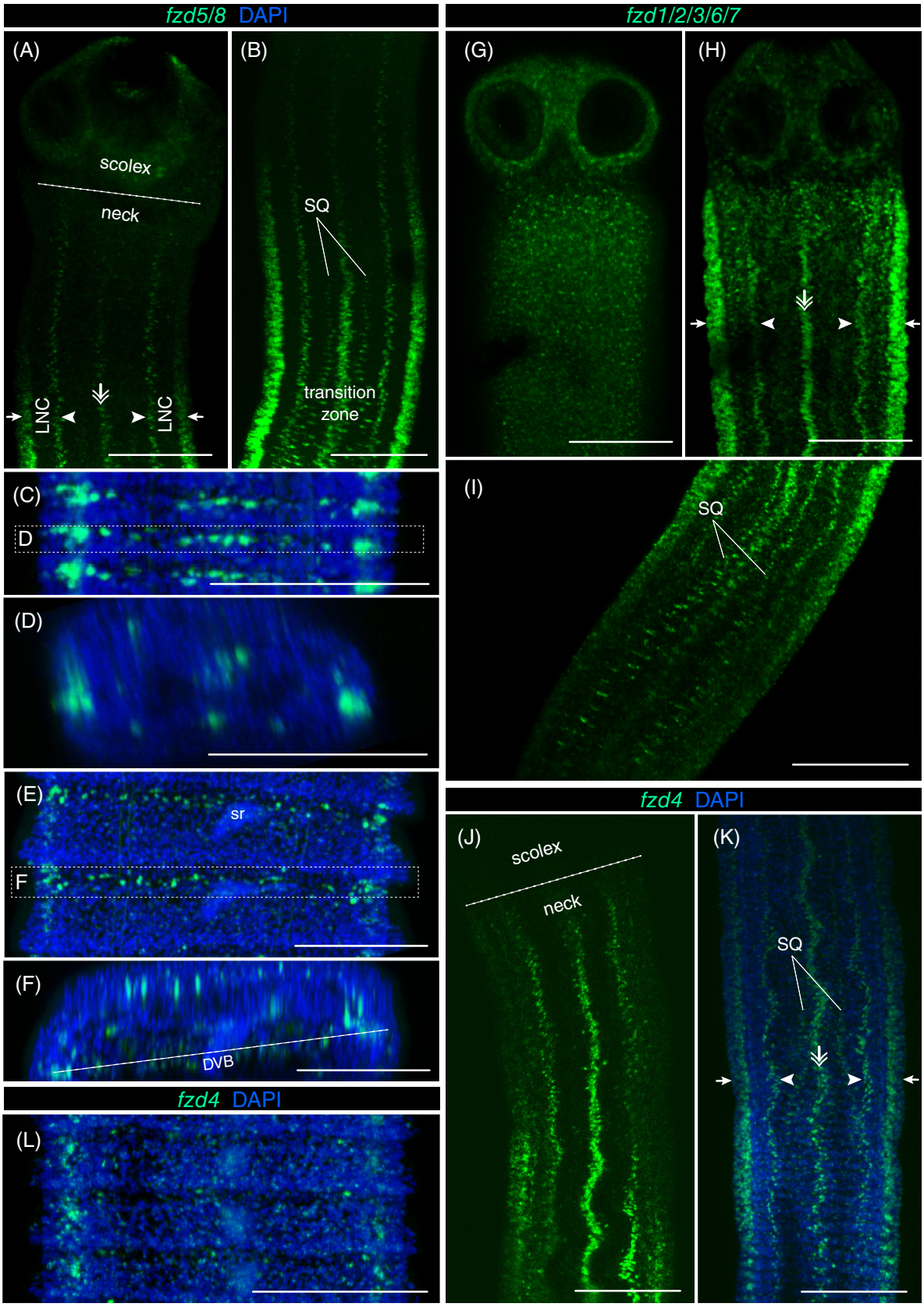

FIGURE 11 Legend on next page.

example of a gene with an especially ephemeral periodicity. Thus, the neck as classically defined is recognizable as a Wnt-inhibitory region, in which several frizzled receptors are expressed in staggered domains and in which a transition zone can be distinguished by the expression domain of *wnt11a*, and by a new, segmental expression domain, the SQ, in which we see the first indications of AP-polarized Wnt expression.

Previous investigation of Wnt signaling during larval development resolved historical questions regarding the polarity of the main body axis,[6] demonstrating that the juvenile worm develops in the anterior (opposite the larval hooks; Figure 1) as conventionally understood.[5] The question of the polarity of their individual segments in relation to the whole worm[7,8] is resolved by the present work showing that segmental boundaries are marked by AP-polarized wnt expression in agreement with the polarity of the main body axis (Figure 8), forming secondary AP axes in each segment. The orientation of the adult body plan is therefore not dissimilar in its head-tail axis to other animals despite reduced cephalization and other adaptations that have confounded anatomical comparison with other animals.

3.3 | The "transition zone" exhibits an embryological character

In planarians, Wnt inhibitors and ligands have been shown to be co-expressed in cells during the initial stages of embryogenesis as well as during the earliest phases of regeneration, in which *sfrp* is expressed prior to co-expression with *wnt1*.[14,52] Co-localization of *wnt1* and the inhibitor *notum* has also been demonstrated during the initial stages of regeneration, prior to their spatial domains becoming AP-polarized.[43] In *H. microstoma*, co-localization of *wnt1* and *sfl* in the SQ shows that Wnt signaling in the transition zone exhibits a character typical of early embryological and regenerative development in flatworms. Also similar to planarians, we find that *sfl* is expressed in the SQ prior to co-expression with *wnt1*.

Morphologically, the onset of strobilation in the transition zone is visible as a field of nascent segments and we have never observed pre-strobilar worms with only a few or a single segment, indicating that strobilation acts across a field of tissues. The expression pattern of *wnt11a* corresponds to a region of the worm that encompasses multiple nascent segments and potentially could act as a trigger to initiate strobilation of the outer body wall. Moreover, being one of two *wnt11* paralogs present in flatworms[18] it may have been free to evolve a novel role in segmentation.

3.4 | Neural expression of *hedgehog* and *sfl* suggests a potential link in signaling

Hedgehog is a secreted signaling protein in bilaterians that is typically expressed in gradients, with receiving cells having a concentration-dependent response.[53,54] It has pleiotropic effects during embryogenesis and is a key player in coordinating the development of the nervous system. In planarians, hedgehog is expressed by differentiated neural cells in the ventral nerve cords and has been shown to have a role in establishing AP polarity by upregulating Wnt signaling.[49,55] Similarly, expression of *hedgehog* in *H. microstoma* is observed in the nervous system, albeit in discrete foci in the cerebral ganglia and at the junctions of the MNCs (Figure 10A,B). It is also expressed in the central medullary region which is likely to represent one of the most cellularly heterogeneous regions that includes myocytons and germinative cells (shown here), peptidergic nerve cells,[32] and most likely many additional cell types including differentiating germinal cell progeny, making it difficult to speculate regarding the identity of *hedgehog*+/*sfl* + cells in this region.[5]

Yazawa et al.[49] proposed that hedgehog proteins in the CNS could be transported posteriorly via axonal trafficking[56] where they are secreted, stimulating Wnt expression in differentiated cells (e.g., myocytes) that in turn signal to neighboring cells, causing upregulation of

FIGURE 11 Frizzled receptor genes show regionalized expression in domains that mirror *sfl*. The three frizzled receptor genes implicated in Wnt signaling all show highly similar domains of expression but differ in their regionalization. *Fzd5/8* (A–F) in particular shows expression in domains that mirror *sfl*, including the marginal myocytons (arrows) and associated foci (arrowheads), central region (double arrow) (A), signaling quartet (SQ, B), the anterior of segments in the strobila (C, E) and along the DV boundary (DVB) at segment boundaries (F). These are all domains seen in *sfl* (Figures 6–8) with the exception of the *sfl* domains associated with the medial longitudinal nerve cords (Figures 6E and 12D). *Fzd5/8* also differs from *sfl* expression in that the foci in the neck become upregulated very gradually (A) until full expression is seen in the transition zone (B). *Fzd1/2/3/6/7* (G-I) shows punctate expression in the outer cortex (G) and the same internal domains of expression as *fzd5/8*, but starting abruptly in the anterior of the neck (H), and fading in the transition zone (I) where it is also expressed in the SQ pattern. *Fzd4* (J, K) shows the same domains at *fzd1/2/3/6/7* but begins more gradually in the neck like *fzd5/8* (J). It is also expressed in punctate pattern in the strobila (L). Scale bars = 100 μm.

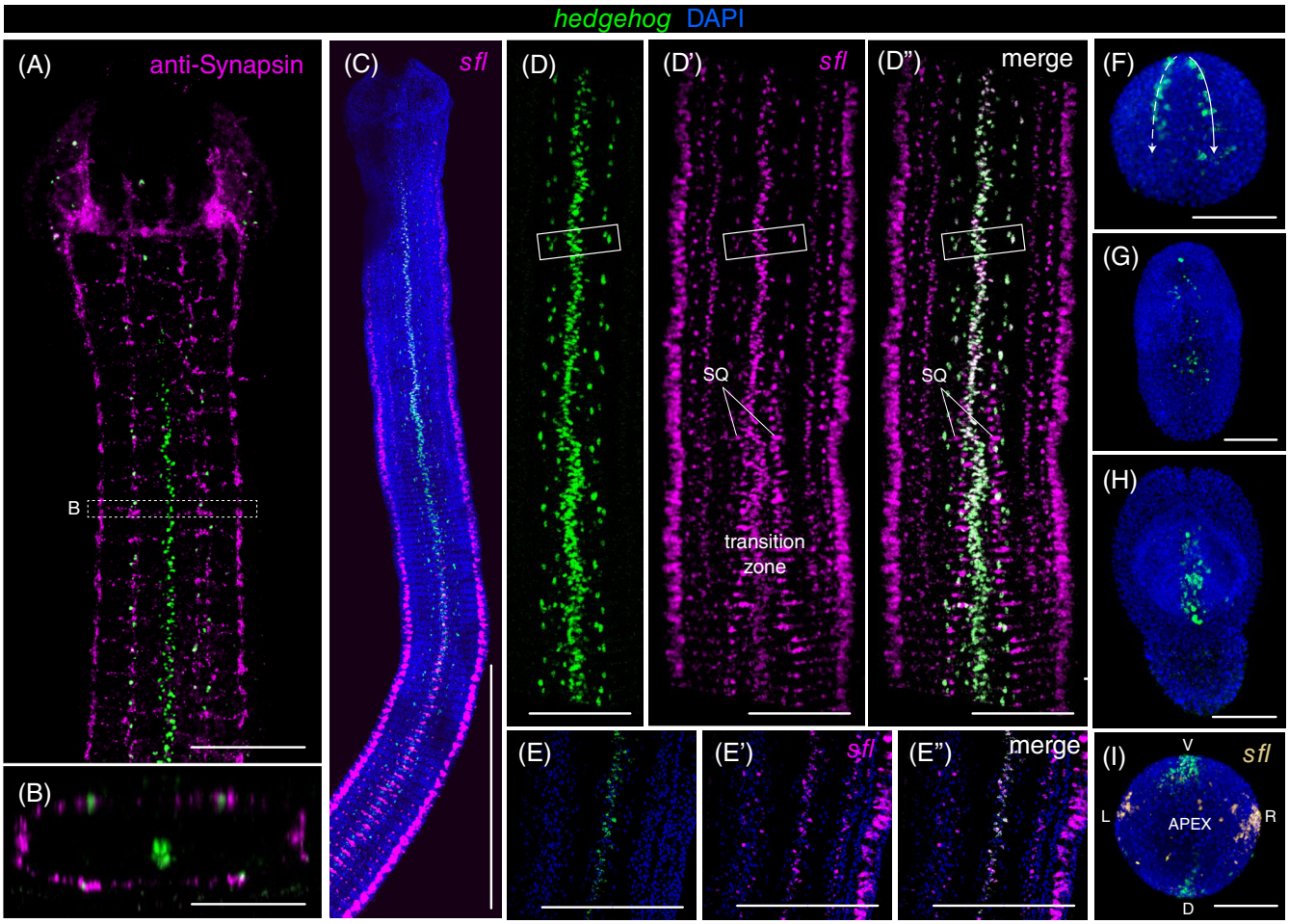

FIGURE 12 *Hedgehog* expression is associated with the nervous system. *Hm-hedgehog* expression in the scolex and neck combined with anti-Synapsin staining of the nervous system (A, B) shows expression at the junctions of the transverse and medial longitudinal nerve cords as well as expression in the central, medullary region. Expression of *hedgehog* combined with *hm-sfl* (C–E) in the neck and transition zone shows co-localization in both the neural-related domains (D, D″, boxes show a single set of foci at a junction) and central region (E, E″). In the transition zone, co-expression with *hedgehog* helps to distinguish the neural domains of *sfl* from the segmentary expression of *sfl* in the signaling quartet (SQ, D″) in which *hedgehog* is not expressed. During larval development, *hedgehog* is expressed along the dorsoventral midlines of the hemisphere that gives rise to the juvenile worm (F–I), whereas *sfl* marks the left (L) and right (R) axes (I). Scale bars = 500 μm in C; 100 μm in A and D–E; 50 μm in B and F–I.

β-catenin and a feedback loop that results in posteriorization. Co-expression of *sfl* and *hedgehog* expression in tapeworms suggests a potential link between hedgehog signaling in the nervous system and Wnt signaling in the musculature, although in the anterior of the worm these systems are not in register with one another and it may be that such a link is first established in the strobila or that neural expression of *sfl* is not related to segmental patterning. The main elements of the nervous system also lie in intimate proximity to both the inner musculature and the germinative cells positioned inside the cortical-medullary boundary (Figure 1E), suggesting that as in planarians, these cells could be directed by signals elicited by the nervous system.

During larval development, *hedgehog* was found to be expressed along the dorsal and ventral midlines, perpendicular to the expression domains of *sfl* that mark the left–right (LR) axes (Figure 8C,D). Midline expression is a conserved feature of hedgehog signaling during embryogenesis that relates to CNS development[50,57] and involvement in planarian neurogenesis has also been demonstrated.[58,59] As with Wnt expression,[5] canonical expression of *hedgehog* during larval metamorphosis in tapeworms is consistent with this representing the phylotypic stage in their ontogeny.[60]

3.5 | Tapeworm segmentation in relation to regeneration in flatworms

The unique combination of the maintenance of somatic stem cells[61] and the continuous expression of PCGs

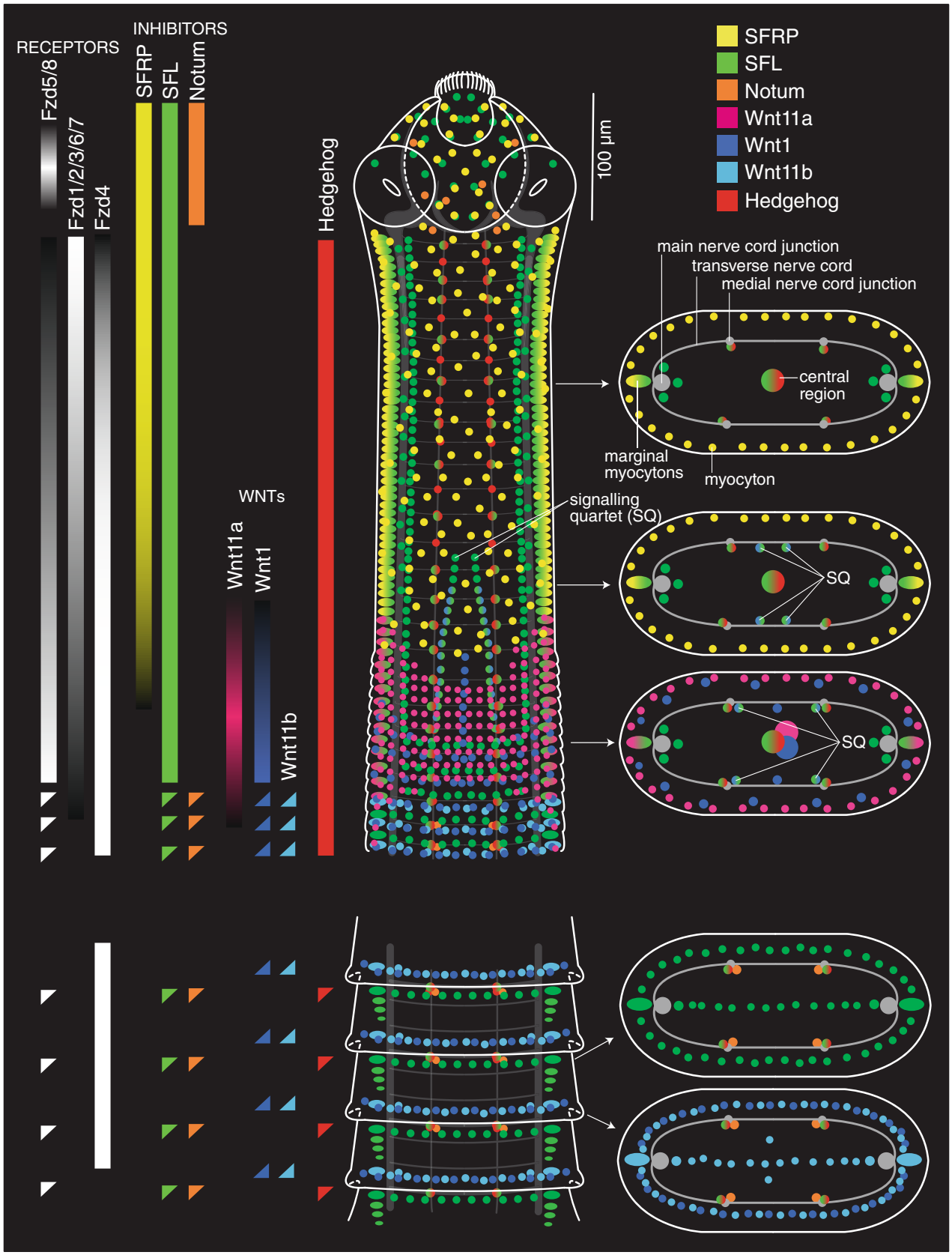

FIGURE 13 Diagram of Wnt and Hedgehog expression domains. Bars show regional expression domains along the anteroposterior (AP) axis while individual foci are shown in the illustration and cross sections. For clarity, the central, medullary domains of expression in the neck region are depicted only in the cross sections. Multicolored foci depict co-localization of factors.

throughout life endows flatworms with extreme developmental plasticity that includes whole-body regeneration in some planarians and widespread abilities of posterior regeneration (i.e., not involving regeneration of the brain) among other free-living groups.[62] In planarians, regeneration involves the formation of new tissues, the blastema, in which a generic wound response is elicited.[63] This is followed by the reestablishment of axial information that induces regeneration of missing tissues through a process of intercalation between the blastema and preexisting tissues,[64] and grafting experiments have shown that new tissues can be intercalated at the AP, DV and LR axes.[64] Almuedo-Castillo et al.[14] extended this model to include homeostasis, or "continuous intercalary respecification," to accommodate the fact that axial patterning systems such as Wnt are perpetually active, even in fully grown, intact flatworms.

The life cycles of parasitic flatworms have evolved to incorporate profound ontogenetic changes that rely on proliferative and transformative growth enabled by somatic stem cells, comparable in many ways to processes of regeneration in free-living flatworms.[47] In tapeworms, adult development is characterized by the continuous intercalation of new tissues in the neck region and involves expression of PCGs canonically associated with AP patterning, suggesting that it can also be viewed as a form of continuous intercalary respecification. Moreover, whereas adult development does not require respecification of axial information or the remodeling of structures, but rather renewed growth of preexisting structures together with the generation of new structures (e.g., TMFs), remodeling of the oncosphere during larval metamorphosis does involve the formation of an entirely new body plan.[38] Thus we suggest that whereas the developmental programs that control larval and adult growth in tapeworms are likely to have evolved independently in the group, they are also likely to share many underlying homologies with gene regulatory networks (GRN) that control development in other parasitic flatworms and the broad spectrum of regenerative abilities in free-living flatworms.

3.6 | Exaptation of a GRN for segmentation

Wnt1, hedgehog, and the homeobox transcription factor Engrailed have been historically canonized as "segment polarity genes."[10,65] Conservation of Wnt–hedgehog interactions in establishing boundaries between adjacent cells is a common mechanism in animals and has been used to infer a common origin of segmentation in bilaterians, or at least in protostomes,[53,66] despite that the underlying modes of segmentation differ within and among groups.[10] Segmentation in tapeworms has been commonly considered an evolutionary novelty,[10] implying a lack of underlying homology to the GRNs of other animals. Planarians and other flatworms, as well as early branching tapeworm lineages, lack segmentation (see below). Nevertheless, AP patterning during planarian regeneration is dependent on hedgehog–Wnt interactions[49,55] with knockdown phenotypes of hedgehog mirroring the AP patterning defects of Wnt/β-catenin.[67,68] Despite their lack of segmentation, the interplay of Wnt and hedgehog in planarian AP patterning has been considered homologous to that of segmented animals.[53] In tapeworms, Wnt and hedgehog expression indicates that they also have a role in establishing and maintaining repeated AP axes along the strobila.[5] Their apparent involvement in polarizing AP boundaries in tapeworms is thus perhaps unexpectedly similar to that of other protostomes, suggesting an underlying homology of their GRN or of specific regulatory modules employed by bilaterians to produce boundaries along the AP axis.[11,69]

The homeobox transcription factor Engrailed has been linked to segmentation perhaps more strongly than any other gene due to the early discovery of its role in forming para-segmental boundaries in *Drosophila*. However, although its function is mostly conserved across arthropods, it varies in other groups suggesting that a role in segmentation is not in fact ancestral.[70] An *H. microstoma* gene model containing an *engrailed*-like homeobox sequence (HmN_003004120) was only recently identified in the complete assembly of its genome[29] and orthologous gene models are found in other parasitic and free-living flatworms. However, RNA-seq quantification in different ontogenetic stages and regions of the *H. microstoma* adult[25,26] demonstrate that it is either not expressed or expressed at levels below minimum thresholds (median 0–1.2 transcripts/million reads) throughout its ontogeny. Thus, although an *engrailed* ortholog is present in *H. microstoma* and broad presence of orthologs across the phylum point to its conservation in parasitic flatworms, lack of expression makes it unlikely to be involved in tapeworm segmentation.

3.7 | Wnt signaling in relation to the evolution of repeated parts and indeterminate growth in tapeworms

Segmentation is the hallmark of tapeworms although not a universally shared feature of the group or one likely to have been present in either the common ancestor or earliest branching lineages of the clade.[2,71] True tapeworms (Eucestoda) are united by a universally observed larval

form (the oncosphere) and other shared, derived characters irrespective of their final body plan. The diversity of extant forms and the phylogenetic pattern of their evolution shows that the segmented body typical of the majority of contemporary species is the result of two evolutionarily and developmentally different processes: repetition of the hermaphroditic sets of reproductive organs (proglottization) and their somatic compartmentalization into semi-discrete segments (strobilation). Although coupled in most groups, there exist forms of tapeworms that are neither proglottized nor segmented (caryophyllideans); proglottized without being segmented (spathebothriideans); have lost segmentation secondarily without accompanying loss of proglottization (*Anantrum*)[71,72]; and are segmented without being proglottized (*Haplobothrium*).[73] These conditions demonstrate the modularity of these processes, including the ability for them to be secondarily decoupled, and phylogenetic analyses point to a possible step-wise pattern of evolution giving rise to the fully segmented condition found in most contemporary forms.[2,71]

Overlaying strobilation on top of proglottization more significantly allowed for indeterminate growth, conferring fully segmented cestodes with at least the theoretical ability for perpetual growth and thus significantly increased reproductive potential. For example, whereas spathebothriidean tapeworms evolved the ability to increase egg production through the development of multiple sets of reproductive organs (proglottization), the number of proglottids they develop is determinate and ultimately restricted by their body size[74] which is in turn restricted by their host. In relation to fully segmented groups, the adults of Spathebothriideans can be viewed as an elongated neck region that undergoes proglottization without accompanying strobilation. The ability to somatically compartmentalize the reproductive organs into segments that could be shed progressively enabled proglottization in more recent groups to proceed indeterminately while the overall body size remained constant.

The existence of these forms considered in light of the present findings suggests a number of questions that merit further investigation. For example, the paired TMFs that define segmental boundaries in *H. microstoma* and that we suggest participate in segmental patterning of the body would not be expected to be observed in tapeworms that lack segmentation and/or proglottization. Similarly, the *wnt11a* paralog whose expression is specifically associated with the onset of strobilation would be expected to play a different role in groups that are not segmented, as could the *sfrp* paralog *sfl* which is linked to segmentation through its expression in the transition zone and strobila. Our work provides a PCG-based framework for addressing these questions through comparative investigations and the development of genomic resources representing most of the exemplar groups discussed above is currently underway.

3.8 | Conclusions

Our findings suggest that segmentation in adult tapeworms could be initiated and guided by the musculature, with new, segmentally repeated elements formed in the neck used to partition the adult body via regionalized and AP-polarized expression of PCGs. Despite profound differences in the trophic and life history strategies of parasitic flatworms, we suggest that the GRNs employed to pattern their bodies are unlikely to differ fundamentally with those of free-living flatworms and other animals. Thus the study of parasitic species throughout the animal kingdom can be instructive not only for understanding unique aspects of their biology and the diseases they cause, but of biology more generally. For example, genomic investigations in parasitic flatworms have revealed that stem cell pluripotency can be maintained in the absence of putatively essential, "universal" multipotency proteins such as Piwi and Vasa[75] that are present in the genomes of free-living flatworms,[76] while complete assembly of the *H. microstoma* genome confirmed for the first time that chromosomes can be capped by centromeres, making these motifs responsible not only for chromosome segregation but also the protection of ends normally conferred by telomeric sequences.[29] Such unexpected findings speak not to the condition of parasitism but to general principles in biology and illustrate the value of broadening the range of organisms that contribute to our understanding of development.[3,77,78]

4 | EXPERIMENTAL PROCEDURES

4.1 | Animals

Adult and larval specimens of the Nottingham strain[20] of *Hymenolepis microstoma* were generated, fixed and stored as previously described.[25] Mice were used in accordance with animal care regulations under UK Home Office license PPL70/8684.

4.2 | Genes and probe synthesis

Gene orthologs were identified from *H. microstoma* genomic data and gene models as previously described.[5,18,21] An isoform of *collagen* was chosen as it was orthologous to the isoform investigated in the planarian *Schmidtea*

mediterranea (Smed_00066_V2).[15] A list of the gene models, primers and protein sequences investigated is given in Additional file 9. Primers were designed against the gene models using Primer3[79] implemented in Geneious (Biomatters Ltd.) and near full-length mRNA transcripts amplified by PCR from cDNAs synthesized from total RNA purified from either larval or adult samples. Amplicons were cloned into StrataClone (Agilent Technologies) or pGEM-T (Promega) vectors and eight positive colonies/gene transferred to 750 µl of ddH2O and heated to 90 C to liberate the plasmids. The size and direction of the inserts were then checked via PCR by combining M13R with GSP forward and reverse primers, and the identities of the inserts confirmed via Sanger sequencing. Insert regions together with flanking T3/T7 or T7/SP6 promotor sites were then amplified in large volume (75 µl) reactions using M13F/R or T7/SP6 primers. Resulting amplicons were used as templates for the synthesis of either digoxigenin (DIG) or fluorescein (FITC)-labeled antisense probes by in vitro transcription using T7 or T3 polymerases (Roche) and DIG or FITC RNA labeling mixes (Roche).

4.3 | Fluorescent in situ hybridization

Larval and adult *H. microstoma* samples were processed in 1.5 ml tubes. Larval samples consisted of mixtures of ~10 specimens each of different larval stages (see Figure 1A) that were processed together. Adult worms were cut into pieces, with samples consisting of ~12 sections of worm/tube representing the scolex and neck and different regions of the strobila of multiple, individual worms. Single FISH was performed on at least two (often many) replicate samples for each factor and some factors (e.g., *hm-sfl*) included many further replicates due to their use for double FISH and/or as positive controls in different runs. Hence, the spatial expression of all factors was assayed in >10 individual specimens/fragments.

Tyramide-FITC-based FISH was performed with DIG-labeled antisense probes as previously described.[5] Double FISH was performed using a modified version of this procedure. During probe hybridization, both DIG and FITC-labeled antisense probes (each at a concentration of 1 µg/ml) were hybridized simultaneously. FITC-labeled probes were detected first by incubating with sheep Anti-Fluorescein-POD Fab fragments (Roche) at a 1:50 dilution. The signal was then developed via tyramide signal amplification (TSA) using a FITC tyramide solution as previously described[5] followed by incubation in 100 mM sodium azide for 45 min to quench the HRP (horseradish peroxidase) enzyme. Samples were then washed four times in PBST (phosphate buffered saline with 1% Tween) for 10 min before incubating in blocking buffer for 1 h. Digoxigenin-labeled probes were detected by incubating with sheep Anti-Digoxigenin-POD Fab fragments (Roche) at a 1:50 dilution. The signal was then developed via TSA using a rhodamine tyramide solution. Specimens were counterstained in DAPI (4′,6-diamidino-2-phenyllindole), cleared in 80% glycerol and wet-mounted on microscope slides.

4.4 | Immunohistochemistry

Phalloidin staining was done on PFA-fixed specimens rinsed in PBS and permeabilized using PBS containing 0.25% TritonX-100 for 2 h. Specimens were stained with AlexaFluor-488 labeled phalloidin (Molecular Probes) in PBS at a final concentration of 1 U/ml. After treatment with Ribonuclease A to remove RNA, nuclear counterstaining was carried out with propidium iodide (1:250) for 20 min. Specimens were rinsed again and mounted on glass slides in 90% glycerol, 10% PBS, and 0.25% DABCO.

Staining with Synapsin was combined with TSA and performed on PFA-fixed specimens permeabilized in 1% sodium dodecyl sulfate (N.B. no Proteinase K treatment) for 1 h prior to the FISH procedure. After FISH detection, specimens were quenched in 100 mM sodium azide to prevent cross-reactivity of the tyramide solutions. Anti-Synapsin (3C11 anti-SYNORF1, Developmental Studies Hybridoma Bank) was used as the primary antibody at a 1:200 dilution. The second antibody was goat-anti-mouse conjugated to HRP. The signal was then amplified via TSA with a rhodamine tyramide solution, as described in the FISH procedure. DAPI (Thermo Fisher) counterstaining was performed last on all specimens by incubating in a 4 ng/ml solution for 10 min.

4.5 | In vitro culture and EdU labeling of cycling cells

To investigate the positions of cycling cells in adult *H. microstoma* we labeled mitotically active cells in vitro with the thymidine analogue 5-ethynyl-2′-deoxyuridine (EdU; Invitrogen). Adult worms were dissected from mice, rinsed in saline with antibiotics and cultured in a supplemented mixture of M199 (Sigma, M2520) culture media in a CO2 incubator as described previously.[27] EdU was added to the culture media at a concentration of 2 µM and after 4 h of exposure, the worms were heat-fixed and preserved for 1 h in 4% paraformaldehyde and detection performed with the Click-iT EdU Alexa Fluor

555 Imaging Kit (Invitrogen). Specimens were then co-labeled via FISH using a probe for *hm-collagen* and counterstained with DAPI.

4.6 | Imaging

Bright-field and fluorescent imaging was done using a Leica DM5000B epifluorescent microscope with CoolLED illumination and a DFC450C digital camera linked to Leica Application Suite ver. 4. Confocal imaging was performed with a Nikon A1-Si confocal microscope and all projections and 3D reconstructions made from resulting image stacks using the Fiji distribution of ImageJ2.[80,81] In some cases, increased differentiation of signals was achieved by adjusting the overall brightness and contrast of different channels.

ACKNOWLEDGMENTS

The authors are grateful to Maximilian Telford (University College London) for providing co-supervisory support to FJ. The authors would like to thank Alex Gruhl for phalloidin staining (Figure 1B), Maria Abellas-Noguerol for anti-Synapsin staining (Figure 1D) and Edward O'Garro-Priddie for generating initial FISH results for *collagen*. The authors would also like to thank Tania Rozario (University of Georgia, USA) for advice on Synapsin and other immunohistochemical stains. The anti-Synapsin hybridoma developed by E. Buchner, University of Würzburg, Germany, was obtained from the Developmental Studies Hybridoma Bank, created by the NICHD of the NIH and maintained at the University of Iowa, Department of Biology, Iowa City, IA 52242.

FUNDING INFORMATION

Francesca Jarero was supported by a PhD fellowship sponsored by the Natural History Museum and University College London.

DATA AVAILABILITY STATEMENT

All genome data are available via WormBase ParaSite (http://parasite.wormbase.org).[82]

ORCID

Andrew Baillie https://orcid.org/0000-0003-3231-4189
Nick Riddiford https://orcid.org/0000-0002-4739-4233
Uriel Koziol https://orcid.org/0000-0002-9699-4964
Peter D. Olson https://orcid.org/0000-0002-4183-4533

REFERENCES

1. Grove DI. *A History of Human Helminthology*. CAB International; 1990:848.
2. Olson PD, Littlewood DTJ, Bray RA, Mariaux J. Interrelationships and evolution of the tapeworms (Platyhelminthes: Cestoda). *Mol Phylogenet Evol*. 2001;19(3):443-467. doi:10.1006/mpev.2001.0930
3. Olson PD. Hox genes and the parasitic flatworms: new opportunities, challenges and lessons from the free-living. *Parasitol Int*. 2008;57(1):8-17. doi:10.1016/j.parint.2007.09.007
4. Koziol U. Evolutionary developmental biology (evo-devo) of cestodes. *Exp Parasitol*. 2017;180:84-100. doi:10.1016/j.exppara.2016.12.004
5. Koziol U, Jarero F, Olson PD, Brehm K. Comparative analysis of Wnt expression identifies a highly conserved developmental transition in flatworms. *BMC Biol*. 2016;14(1):10. doi:10.1186/s12915-016-0233-x
6. Stunkard HW. The organization, ontogeny, and orientation of the Cestoda. *Q Rev Biol*. 1962;37(1):23-34. doi:10.2307/2816742
7. Minelli A. The tapeworm's elusive antero-posterior polarity. *BMC Biol*. 2016;14(1):1-3. doi:10.1186/s12915-016-0244-7
8. Egger B. Making heads or tails of tapeworms. *Trends Parasitol*. 2016;32(7):511-512. doi:10.1016/j.pt.2016.04.003
9. Young RT. Some unsolved problems of cestode structure and development. *Trans Am Microsc Soc*. 1935;54(3):229-239. doi:10.2307/3222135
10. Blair SS. Segmentation in animals. *Curr Bio*. 2008;18(21):R991-R995. doi:10.1016/j.cub.2008.08.029
11. Vellutini BC. Segmental traits in non-segmented Bilaterians. In: Chipman AD, ed. *Cellular Processes in Segmentation*. CRC Press; 2020:205-253.
12. Petersen CP, Reddien PW. Wnt signaling and the polarity of the primary body axis. *Cell*. 2009;139(6):1056-1068. doi:10.1016/j.cell.2009.11.035
13. Petersen CP, Reddien PW. A wound-induced Wnt expression program controls planarian regeneration polarity. *Proc Natl Acad Sci U S A*. 2009;106(40):17061-17066. doi:10.1073/pnas.0906823106
14. Almuedo-Castillo M, Sureda-Gómez M, Adell T. Wnt signaling in planarians: new answers to old questions. *Int J Dev Biol*. 2012;56(1-2-3):53-65. doi:10.1387/ijdb.113451ma
15. Witchley JN, Mayer M, Wagner DE, Owen JH, Reddien PW. Muscle cells provide instructions for planarian regeneration. *Cell Rep*. 2013;4(4):633-641. doi:10.1016/j.celrep.2013.07.022
16. Scimone ML, Cote LE, Reddien PW. Orthogonal muscle fibres have different instructive roles in planarian regeneration. *Nature*. 2017;126:1-22. doi:10.1038/nature24660
17. Niehrs C. On growth and form: a Cartesian coordinate system of Wnt and BMP signaling specifies bilaterian body axes. *Development*. 2010;137(6):845-857. doi:10.1242/dev.039651
18. Riddiford N, Olson PD. Wnt gene loss in flatworms. *Dev Genes Evol*. 2011;221(4):187-197. doi:10.1007/s00427-011-0370-8
19. Chervy L. The terminology of larval cestodes or metacestodes. *Syst Parasitol*. 2002;52:1-33.
20. Cunningham LJ, Olson PD. Description of *Hymenolepis microstoma* (Nottingham strain): a classical tapeworm model for research in the genomic era. *Parasit Vectors*. 2010;3:123. doi:10.1186/1756-3305-3-123
21. Tsai IJ, Zarowiecki M, Holroyd N, et al. The genomes of four tapeworm species reveal adaptations to parasitism. *Nature*. 2013;496(7443):57-63. doi:10.1038/nature12031
22. International Helminth Genomes Consortium. Comparative genomics of the major parasitic worms. *Nat Genet*. 2019;51(1):163-174. doi:10.1038/s41588-018-0262-1

23. Macchiaroli N, Cucher M, Kamenetzky L, et al. Identification and expression profiling of microRNAs in Hymenolepis. *Int J Parasitol*. 2019;49(3–4):211-223. doi:10.1016/j.ijpara.2018.07.005
24. James K, Olson PD. The tapeworm interactome: inferring confidence scored protein-protein interactions from the proteome of *Hymenolepis microstoma*. *BMC Genomics*. 2020;21(1):1-22. doi:10.1186/s12864-020-6710-1
25. Olson PD, Zarowiecki M, James K, et al. Genome-wide transcriptome profiling and spatial expression analyses identify signals and switches of development in tapeworms. *EvoDevo*. 2018;9(1):1-29. doi:10.1186/s13227-018-0110-5
26. Preza M, Calvelo J, Langleib M, et al. Stage-specific transcriptomic analysis of the model cestode *Hymenolepis microstoma*. *Genomics*. 2021;113(2):620-632. doi:10.1016/j.ygeno.2021.01.005
27. Pouchkina-Stantcheva NN, Cunningham LJ, Hrčkova G, Olson PD. RNA-mediated gene suppression and in vitro culture in *Hymenolepis microstoma*. *Int J Parasitol*. 2013;43:641-646. doi:10.1016/j.ijpara.2013.03.004
28. Montagne J, Preza M, Koziol U. Stem cell proliferation and differentiation during larval metamorphosis of the model tapeworm *Hymenolepis microstoma*. *Front Cell Infect Microbiol*. 2023;13:1286190. doi:10.1101/2023.09.13.557592
29. Olson PD, Tracey A, Baillie A, et al. Complete representation of a tapeworm genome reveals chromosomes capped by centromeres, necessitating a dual role in segregation and protection. *BMC Biol*. 2020;18(1):1-16. doi:10.1186/s12915-020-00899-w
30. Rozario T, Newmark PA. A confocal microscopy-based atlas of tissue architecture in the tapeworm *Hymenolepis diminuta*. *Exp Parasitol*. 2015;158:31-41. doi:10.1016/j.exppara.2015.05.015
31. Halton DW, Maule AG. Flatworm nerve-muscle: structural and functional analysis. *Can J Zool*. 2004;82(2):316-333. doi:10.1139/z03-221
32. Preza M, Bael SV, Temmerman L, Guarnaschelli I, Castillo E, Koziol U. Global analysis of neuropeptides in cestodes identifies Attachin, a SIFamide homolog, as a stimulant of parasite motility and attachment. *J Neurochem*. 2022;162:467-482. doi:10.1111/jnc.15654
33. Koziol U, Costábile A, Domínguez MF, et al. Developmental expression of high molecular weight tropomyosin isoforms in *Mesocestoides corti*. *Mol Biochem Parasitol*. 2011;175(2):181-191. doi:10.1016/j.molbiopara.2010.11.009
34. Koziol U, Rauschendorfer T, Rodríguez LZ, Brehm K. The unique stem cell system of the immortal larva of the human parasite *Echinococcus multilocularis*. *EvoDevo*. 2014;5(10):1-23. doi:10.1186/2041-9139-5-10
35. Sulgostowska T. The development of organ systems in cestodes. I. A study of histology of *Hymenolepis diminuta* (Rudolphi, 1819) (Hymenolepididae). *Acta Parasitol Polonica*. 1972;20(37):449-462. http://scholar.google.com/scholar?q=related:Fx675bpfcyQJ:scholar.google.com/&hl=en&num=20&as_sdt=0,5
36. Sulgostowska T. The development of organ systems in cestodes. II. Histogenesis of the reproductive system in Hymenolepis diminuta (Rudolphi, 1819) (Hymenolepididae). *Acta Parasitol Polonica*. 1974;22(16):179-190. http://scholar.google.com/scholar?q=related:b9bcA3hWwUoJ:scholar.google.com/&hl=en&num=20&as_sdt=0,5
37. Cote LE, Simental E, Reddien PW. Muscle functions as a connective tissue and source of extracellular matrix in planarians. *Nat Commun*. 2019;10(1):1-13. doi:10.1038/s41467-019-09539-6
38. Montagne J, Preza M, Koziol U. Stem cell proliferation and differentiation during larval metamorphosis of the model tapeworm *Hymenolepis microstoma*. *Front Cell Infect Microbiol*. 2023;13:1-13. doi:10.3389/fcimb.2023.1286190
39. Caley J. The functional significance of scolex retraction and subsequent cyst formation in the cysticercoid larva of *Hymenolepis microstoma*. *Parasitology*. 1974;68(2):207-227. doi:10.1017/s0031182000045741
40. Kakugawa S, Langton PF, Zebisch M, et al. Notum deacylates Wnt proteins to suppress signalling activity. *Nature*. 2015;519(7542):187-192. doi:10.1038/nature14259
41. Zhang X, Cheong SM, Amado NG, et al. Notum is required for neural and head induction via Wnt deacylation, oxidation, and inactivation. *Dev Cell*. 2015;32(6):719-730. doi:10.1016/j.devcel.2015.02.014
42. Roberts-Galbraith RH, Newmark PA. Follistatin antagonizes activin signaling and acts with notum to direct planarian head regeneration. *Proc Natl Acad Sci U S A*. 2013;110(4):1363-1368. doi:10.1073/pnas.1214053110
43. Petersen CP, Reddien PW. Polarized notum activation at wounds inhibits Wnt function to promote planarian head regeneration. *Science*. 2011;332(6031):852-855. doi:10.1126/science.1202143
44. Hill EM, Petersen CP. Wnt/notum spatial feedback inhibition controls neoblast differentiation to regulate reversible growth of the planarian brain. *Development*. 2015;142(24):4217-4229. doi:10.1242/dev.123612
45. Range RC. Canonical and non-canonical Wnt signaling pathways define the expression domains of frizzled 5/8 and frizzled 1/2/7 along the early anterior-posterior axis in sea urchin embryos. *Dev Biol*. 2018;444(2):83-92. doi:10.1016/j.ydbio.2018.10.003
46. Scimone ML, Cote LE, Rogers T, Reddien PW. Two FGFRL-Wnt circuits organize the planarian anteroposterior axis. *eLife*. 2016;5:e12845. doi:10.7554/elife.12845
47. Rozario T, Quinn EB, Wang J, Davis RE, Newmark PA. Region-specific regulation of stem cell-driven regeneration in tapeworms. *Elife*. 2019;8:77. doi:10.7554/elife.48958
48. Pascual-Carreras E, Sureda-Gómez M, Barrull-Mascaró R, et al. WNT-FRIZZLED-LRP5/6 signaling mediates posterior fate and proliferation during planarian regeneration. *Genes*. 2021;12(1):101-114. doi:10.3390/genes12010101
49. Yazawa S, Umesono Y, Hayashi T, Tarui H, Agata K. Planarian hedgehog/patched establishes anterior-posterior polarity by regulating Wnt signaling. *Proc Natl Acad Sci U S A*. 2009;106(52):22329-22334. doi:10.1073/pnas.0907464106
50. Rétaux S, Kano S. Midline signaling and evolution of the forebrain in chordates: a focus on the lamprey hedgehog case. *Integr Comp Biol*. 2010;50(1):98-109. doi:10.1093/icb/icq032
51. Sureda-Gomez M, Adell T. Planarian organizers. *Semin Cell Dev Biol*. 2018;87:95-104. doi:10.1016/j.semcdb.2018.05.021
52. Martín-Durán JM, Amaya E, Romero R. Germ layer specification and axial patterning in the embryonic development of the freshwater planarian *Schmidtea polychroa*. *Dev Biol*. 2010;340(1):145-158. doi:10.1016/j.ydbio.2010.01.018
53. Ingham PW, Nakano Y, Seger C. Mechanisms and functions of hedgehog signalling across the metazoa. *Nat Rev Genet*. 2011;12(6):393-406. doi:10.1038/nrg2984

54. Hooper JE, Scott MP. Communicating with hedgehogs. *Nat Rev Mol Cell Biol*. 2005;6(4):306-317. doi:10.1038/nrm1622
55. Rink JC, Gurley KA, Elliott SA, Alvarado AS. Planarian Hh signaling regulates regeneration polarity and links Hh pathway evolution to cilia. *Science*. 2009;326(5958):1406-1410. doi:10.1126/science.1178712
56. Daniele JR, Baqri RM, Kunes S. Analysis of axonal trafficking via a novel live-imaging technique reveals distinct hedgehog transport kinetics. *Biol Open*. 2017;6(5):714-721. doi:10.1242/bio.024075
57. Neuhaus-Follini A, Bashaw GJ. Crossing the embryonic midline: molecular mechanisms regulating axon responsiveness at an intermediate target. *WIREs Dev Bio*. 2015;4(4):377-389. doi:10.1002/wdev.185
58. Currie KW, Molinaro AM, Pearson BJ. Neuronal sources of hedgehog modulate neurogenesis in the adult planarian brain. *Elife*. 2016;5:e19735. doi:10.7554/elife.19735
59. Wang IE, Lapan SW, Scimone ML, Clandinin TR, Reddien PW. Hedgehog signaling regulates gene expression in planarian glia. *Elife*. 2016;5:905. doi:10.7554/elife.16996
60. Levin M, Anavy L, Cole AG, et al. The mid-developmental transition and the evolution of animal body plans. *Nature*. 2016;531(7596):637-641. doi:10.1038/nature16994
61. Peter R, Gschwentner R, Schürmann W, Rieger RM, Ladurner P. The significance of stem cells in free-living flatworms: one common source for all cells in the adult. *J App Biomed*. 2004;2:21-35. http://www.uibk.ac.at/zoology/staff/egger/images/images/peter-macrostomum-neoblasts-2004.pdf
62. Cebrià F, Saló E, Adell T. Regeneration and growth as modes of adult development: the Platyhelminthes as a case study. *Evolutionary Developmental Biology of Invertebrates 2: Lophotrochozoa*. Springer; 2015:41-78. doi:10.1007/978-3-7091-1871-9_4
63. Wurtzel O, Cote LE, Poirier A, Satija R, Regev A, Reddien PW. A generic and cell-type-specific wound response precedes regeneration in planarians. *Dev Cell*. 2015;35(5):632-645. doi:10.1016/j.devcel.2015.11.004
64. Agata K, Tanaka T, Kobayashi C, Katoh K, Saitoh Y. Intercalary regeneration in planarians. *Dev Dyn*. 2003;226(2):308-316. doi:10.1002/dvdy.10249
65. Chipman A. Parallel evolution of segmentation by co-option of ancestral gene regulatory networks. *Bioessays*. 2010;32(1):60-70.
66. Dray N, Tessmar-Raible K, Gouar ML, et al. Hedgehog signaling regulates segment formation in the annelid Platynereis. *Science*. 2010;329(5989):339-342. doi:10.1126/science.1188913
67. Petersen CP, Reddien PW. Smed-betacatenin-1 is required for anteroposterior blastema polarity in planarian regeneration. *Science*. 2008;319(5861):327-330. doi:10.1126/science.1149943
68. Gurley KA, Rink JC, Alvarado AS. Smed-βcatenin-1 defines head versus tail identity during planarian regeneration and homeostasis. *Science*. 2008;319(5861):323-327. doi:10.1126/science.1150029
69. Vellutini BC, Hejnol A. Expression of segment polarity genes in brachiopods supports a non-segmental ancestral role of engrailed for bilaterians. *Sci Rep*. 2016;6:1-16. doi:10.1038/srep32387
70. Iyer H, Collins JJI, Newmark PA. NF-YB regulates spermatogonial stem cell self-renewal and proliferation in the planarian *Schmidtea mediterranea*. *PLoS Genet*. 2016;12(6):e1006109-e1006118. doi:10.1371/journal.pgen.1006109
71. Olson PD, Poddubnaya L, Littlewood DTJ, Scholz T. On the position of Archigetes and its bearing on the early evolution of the tapeworms. *J Parasitol*. 2008;94(4):898-904.
72. Overstreet RM. Parasites of the inshore lizardfish, *Synodus foetens*, from south Florida, including a description of a new genus of Cestoda. *Bull Mar Sci*. 1968;2(18):445-470.
73. Cooper AR. A new cestode from *Amia calva* L. *Trans Royal Canad Inst*. 1915;X:81-120.
74. Marques JF, Santos MJ, Gibson DI, Cabral HN, Olson PD. Cryptic species of Didymobothrium rudolphii (Cestoda: Spathebothriidea) from the sand sole, Solea lascaris, off the Portuguese coast, with an analysis of their molecules, morphology, ultrastructure and phylogeny. *Parasitology*. 2007;134(7):1057-1072. doi:10.1017/s0031182007002491
75. Juliano CE, Swartz SZ, Wessel GM. A conserved germline multipotency program. *Development*. 2010;137(24):4113-4126. doi:10.1242/dev.047969
76. Skinner DE, Rinaldi G, Koziol U, Brehm K. How might flukes and tapeworms maintain genome integrity without a canonical piRNA pathway? *Trends Parasitol*. 2014;30(3):123-129. doi:10.1016/j.pt.2014.01.001
77. Alvarado AS. To solve old problems, study new research organisms. *Dev Biol*. 2018;433(2):111-114. doi:10.1016/j.ydbio.2017.09.018
78. Rozario T, Collins JJ, Newmark PA. The good, the bad, and the ugly: from planarians to parasites. *Curr Top Dev Biol*. 2022;147:345-373. doi:10.1016/bs.ctdb.2021.12.015
79. Untergasser A, Cutcutache I, Koressaar T, et al. Primer3—new capabilities and interfaces. *Nucleic Acids Res*. 2012;40(15):e115. doi:10.1093/nar/gks596
80. Schindelin J, Arganda-Carreras I, Frise E, et al. Fiji: an open-source platform for biological-image analysis. *Nat Methods*. 2012;9(7):676-682. doi:10.1038/nmeth.2019
81. Rueden CT, Schindelin J, Hiner MC, et al. ImageJ2: ImageJ for the next generation of scientific image data. *BMC Bioinform*. 2017;18(1):529. doi:10.1186/s12859-017-1934-z
82. Howe KL, Bolt BJ, Shafie M, Kersey P, Berriman M. WormBase ParaSite – a comprehensive resource for helminth genomics. *Mol Biochem Parasitol*. 2017;215:2-10. doi:10.1016/j.molbiopara.2016.11.005

SUPPORTING INFORMATION

Additional supporting information can be found online in the Supporting Information section at the end of this article.

How to cite this article: Jarero F, Baillie A, Riddiford N, Montagne J, Koziol U, Olson PD. Muscular remodeling and anteroposterior patterning during tapeworm segmentation. *Developmental Dynamics*. 2024;253(11):998-1023. doi:10.1002/dvdy.712